



รายงานวิจัยฉบับสมบูรณ์

โครงการ

การพัฒนาตัวเร่งปฏิกิริยาที่ประกอบด้วยเฟอร์โรซีนสำหรับ ปฏิกิริยาพอลิเมอร์ ไรเซชันแบบอนุมูลอิสระถ่ายโอนอะตอม

> โดย รองศาสตราจารย์ เอกสิทธิ์ สมสุข

> > เดือนมิถุนายน 2556

รายงานวิจัยฉบับสมบูรณ์

โครงการ

การพัฒนาตัวเร่งปฏิกิริยาที่ประกอบด้วยเฟอร์โรซีนสำหรับ ปฏิกิริยาพอลิเมอร์ ไรเซชันแบบอนุมูลอิสระถ่ายโอนอะตอม

โดย

รองศาสตราจารย์ เอกสิทธิ์ สมสุข ภาควิชาเคมี คณะวิทยาศาสตร์ มหาวิทยาลัยมหิดล

สนับสนุนโดยสำนักงานกองทุนสนับสนุนการวิจัย และ สำนักงานคณะกรรมการการอุดมศึกษา (ความเห็นในรายงานนี้เป็นของผู้วิจัย สกว. ไม่จำเป็นต้องเห็นด้วยเสมอไป) รูปแบบ Abstract (บทคัดย่อ)

Project Code: RMU5380043

Project Title: การพัฒนาตัวเร่งปฏิกิริยาที่ประกอบด้วยเฟอร์โรซีนสำหรับปฏิกิริยาพอลิเมอร์ไรเซชัน

แบบอนุมูลอิสระถ่ายโอนอะตอม

ชื่อนักวิจัย และสถาบัน

รองศาสตราจารย์ เอกสิทธิ์ สมสุข ภาควิชาเคมี คณะวิทยาศาสตร์ มหาวิทยาลัยมหิดล

E-mail Address: Ekasith.som@mahidol.ac.th

Project Period: 3 1

Abstract

The polymerization of methyl methacrylate (MMA) catalyzed by CuBr/tris(2-(ferrocenyl

methylamino)ethyl)amine unexpectedly proceeded in the absence of alkyl halide. The

growth of molecular weight and the conversion were linearly dependent indicating the

living character of radical polymerization process. Reaction between CuBr and tris(2-

(ferrocenyl methylamino)ethyl)amine showed the formation of Cu(II) as evidenced from

electron paramagnetic resonance (EPR) study. Moreover, the radical trapping by

(2,2,6,6-tetramethyl-piperidin-1-yl)oxyl (TEMPO) and the deuterated labeling ligand in

the presence of CuBr indicated that the polymerization proceeded via a radical

mechanism.

KEYWORDS: Ferrocene; Tripodal Ligand; Radical Polymerization

บทคัดย่อ

ปฏิกิริยาพอลิเมอไรเซชันของ methyl methacrylate (MMA) โดยมี CuBr/tris(2-(ferrocenyl

methylamino)ethyl)amine เป็นตัวเร่งปฏิกิริยา เกิดขึ้นได้โดยไม่มี alkyl halide. การเพิ่มขึ้นของ

molecular weight และ conversion มีความสัมพันธ์เป็นเส้นตรงซึ่งเป็นลักษณะของ living

character of radical polymerization process ปฏิกิริยาระหว่าง CuBr and tris(2-(ferrocenyl

methylamino)ethyl)amine แสดงว่าเกิด Cu(II) ซึ่งยืนยันจาก electron paramagnetic resonance

(EPR) และ การทดลอง radical trapping ของ (2,2,6,6-tetramethyl-piperidin-1-yl)oxyl (TEMPO)

ที่มี deuterated labeling ligand และ CuBr บ่งบอกว่าปฏิกิริยานี้เกิดผ่าน radical mechanism.

KEYWORDS: Ferrocene; Tripodal Ligand; Radical Polymerization

Output จากโครงการวิจัยที่ได้รับทุนจาก สกว.

- 1. ผลงานตีพิมพ์ในวารสารวิชาการนานาชาติ
 - a. Win Mar, W.; Somsook, E.* "Esterification of fatty acid catalyzed by hydrothermally stable propylsulfonic acid-functionalized mesoporous silica SBA-15" *J. Oleo Sci.* **2013**, *62*, 435-442.
 - b. Chaicharoenwimolkul, L.; Chairam, S.; Namkajorn, M.; Khamthip, A.; Kamonsatikul, C.; Tewasekson, U.; Jindabot, S.; Pon-On, W.; Somsook, E.* "Effect of Ferrocene Substituents and Ferricinium Additive on the Properties of Polyaniline Derivatives and Catalytic Activities of Palladium-Doped Poly(*m*-ferrocenylaniline)-catalyzed Suzuki-Miyaura Cross-coupling Reactions" *J. Appl. Polym. Sci.* **2013**, *130*, 1489-1497.

2. ผลงานที่คาดว่าจะเผยแพร่หลังจากนี้

- a. Unexpected self-initiated polymerization of methyl methacrylate by using Cu(I)/N-tripodal ligand with ferrocene moieties as catalyst.
- 3. ผลงานตีพิมพ์ในวารสารวิชาการนานาชาติ (ที่ร่วมมือกับทุนวิจัยอื่นหรือนักวิจัยท่านอื่น)
 - a. Munmai, A.; Ruenwongsa, P.; Panijpan, B.; Barman, N.; Magee, P. A.; Somsook, E.* "Using Principles of Subtractive Colors to Teach Color of Pigments" *Int. J. Learning* **2011**, *18*, 203-218.
 - b. Win Mar, W.; **Somsook, E.*** "Biomass-based sulfonic-functionalized carbon solid acid for esterification of acetic acid" *Adv. Mater. Res.* **2012**, *506*, 70-73.
 - c. Chairam, S.*; Sriraksa, W.; Amatatongchai, M.; **Somsook, E.** "Electrocatalytic Oxidation of Ascorbic Acid using a Poly(aniline-*co-m*-ferrocenylaniline) Modified Glassy Carbon Electrode" Sensors **2011**, *11*, 10166-10179.
 - d. Munmai, A.; **Somsook, E.*** "The Determination of the pK_a of Red Cabbage Anthocyanin by the Spectrophotometric Method and Nonlinear Curve Fitting" *Chem. Educ.* **2011**, *16*, 323-325.
 - e. Win Mar, W.; Somsook, E.* "Methanolysis of Soybean Oil over KCl/CaO Solid Base Catalyst for Biodiesel Production" *ScienceAsia* **2012**, *38*, 90-94
 - f. Win Mar, W.; Somsook, E.* "Sulfonic-Functionalized Carbon Catalyst for Esterification of High Free Fatty Acid" *Proc. Eng.* **2012**, *32*, 212-218.
 - g. Kamonsatikul, C.; Khamnaen, T.; Phiriyawirut, P.; Charoenchaidet, S.; Somsook, E.* "Synergistic Activities of Magnetic Nanoparticles and Stabilizing Ligands Containing Ferrocene Moieties in Selective Oxidation of Benzyl Alcohol" *Catal. Commun.* **2012**, *26*, 1-5.
 - h. Kaewmati, P.; Somsook, E.*, Dhital, R. N.; Sakurai, H. "Aerobic oxygenation of phenylboronic acid promoted by thiol derivatives under gold-free conditions: a warning against gold nanoparticle catalysis" *Tetrahedron Lett.* **2012**, *53*, 6104-6106.
 - i. Jaroentomeechai, T.; Yingsukkamol, P.; Phurat, C.; Somsook, E.; Osotchan, T.; Ervithayasuporn, V.* "Synthesis and reactivity of nitrogen nucleophiles-induced cage-rearrangement silsesquioxanes" *Inorg. Chem.* **2012**, *51*, 12266-12272.

- j. Dhital, R. N.; Kamonsatikul, C.; Somsook, E.; Bobuatong, K.; Ehara, M.; Karanjit, S.; Sakurai, H.* "Low-temperature Carbon-Chlorine Bond Activation by Bi-metallic Gold/Palladium Alloy Nanoclusters: An Application to Ullmann Coupling" *J. Am. Chem. Soc.* 2012, 134, 20250-20253.
- k. Sangtrirutnugul, P.*; Maisopa, P.; Chaicharoenwimolkul, L.; Sunsin, A.; Somsook, E.; Reutrakul, V. "Tripodal "Click" Ligand for Copper-Catalyzed ATRP *J. Appl. Polym. Sci.* **2013**, *127*, 2757-2763.
- 1. Dhital, R. N.; Kamonsatikul, C.; Somsook, E.; Sato, Y.; Sakurai, H.* "Aryl Iodides as Strong Inhibitor in Gold and Gold-Based Bimetallic quasi-Homogeneous Catalysis" *Chem. Commun.* **2013**, 2542-2544.
- m. Ervithayasuporn, V.*; Sodkhomkhum, R.; Teerawatananond, T.; Phurat, C.; Phinyocheep, P.; Somsook, E.; Osotchan, T. "Unprecedented Formation of *cis* and *trans*-Di[(3-chloropropyl)isopropoxysilyl]-Bridged Double-Decker Octaphenylsilsesquioxanes" *Eur. J. Inorg. Chem.* in press.
- n. Dhital, R. N.; Kamonsatikul, C.; Somsook, E.; Sakurai, H.* "Bimetallic Gold/Palladium Alloy Nanoclusters: An Effective Catalyst for Ullmann Coupling of Chloropyridines under Ambient Conditions" *Catal. Sci. Tech.* in press.

4. การเสนอผลงานในที่ประชุมวิชาการ

Invited Presentations	
October 12, 2011	"The selectivities and catalytic activities enhancements by catalysts containing ferrocene moieties" at the 37 th -STT,
	Bangkok.
November 10, 2011	"Catalytic Reactions for Biorefineries and Petrochemical
1,0,0,110,110,111	Industries" at Ubon Ratchathani University
May 2, 2012	"Nanocast in Nanocatalysis" at Department of Chemistry,
3	Faculty of Science, Mahidol University
August 9-10, 2012	"Olefin Polymerization Catalysis" at Thai Polyethylene Co.,
	Ltd., Rayong, Thailand
September 18, 2012	"Solid-State NMR Workshop" at Siam Research and
	Innovation, Saraburi, Thailand
October 28, 2012	"Chemistry" at Science Camp, National Science Museum,
	Pathumthani, Thailand
July 26, 2013	"Chemical Safety in Laboratory" at Faculty of Science,
	Mahidol University
August 22, 2013	"Synergistic Activities of Magnetic Iron-Oxide
	Nanoparticles and Stabilizing Ligands Containing Ferrocene
	Moieties in Selective Oxidation of Benzyl Alcohol" at 15 th
	Asian Chemical Congress at Resort World Sentosa,
	Singapore
Oral Presentations	
October 28, 2011	"Enhance Thai Student Learning of Chemical Kinetics by
October 28, 2011	Eggshell Experiment" at the 3 rd -Asian Conference on
	Education at Osaka, Japan
	Zaranian an Obumu, vapan

June 14, 2012	"Synthesis and Characterization of Solid Base Catalysts Based on Waste Eggshell as Reactant Template for Incorporation of CaCl ₂ and KF and Their Catalytic Activities in the Transesterification of Soybean Oil" at the 2 nd -Korean- Indonesia Workshop and International Symposium on Bioenergy from Biomass (Keynote Speaker)
June 22, 2012	"Synergistic Activities of Magnetic Iron-Oxide Nanoparticles and Stabilizing Ligands Containing Ferrocene Moieties in Selective Oxidation of Benzyl Alcohol" at International Functional Molcules & Materials Meeting at Walailak University (Keynote Speaker)
September 7, 2012	"Demetallation of Ferrocene Boronic Acid Catalyzed by Gold Catalysts" at the 25 th International Conference on Organometallic Chemistry at Lisbon, Portugal
October 1 st , 2012	"Transesterification of soybean oil to biodiesel by solid base catalyst derived from mixing potassium fluoride and calcium nitrate assisted by vermicelli as a template" at the World Congress on Oleo Science at Sasebo, Nagasaki, Japan
October 10 th , 2012	"Atom Transfer Radical Polymerization Catalyzed by Copper Catalysts Containing Ferrocene Moieties" at TRF Annual Meeting at Cha-Am, Thailand
October 19 th , 2012	"Demetallation of Ferrocene Boronic Acid Catalyzed by Gold Catalysts" at the 38 th STT-Conference on Science and Technology of Thailand at Chiang Mai, Thailand
Poster Presentations	
May 29-31, 2011	"Effect of Ferrocene Moieties on Copper-Based Atom Transfer Radical Polymerization of Methyl Methacrylate" at the 2 nd -Frontiers in Polymer Science at Lyon, France.
October 2-5, 2011	"Transesterification of soybean oil to biodiesel by solid base catalyst derived from mixing potassium fluoride and calcium nitrate assisted by vermicelli as a template" at the 1 st -CatBior at Malága, Spain
December 4-8, 2011	"Self-initiation Radical Polymerization of Methyl Methacrylate Catalyzed by Cu(I)/Tripodal Ligand with Ferrocene Moieties" at 2011 Catalysis & Fine Chemicals Symposium at Nara, Japan
March 27-30, 2012	"Iron Oxide-Starch Nanocomposite Catalysts for Olefin Polymerization" at 8 th -International Colloquium on Ziegler- Natta Heterogeneous Catalysts at Kanazawa, Japan

July 8-11, 2012	"Upgrading FAME Derived Coconut Oil into Useful Chemicals and Higher Volatile Biofuels by Simple Chemical Pathways at CAT4BIO: Advanced in Catalysis for Biomass Valorization at Thessaloniki, Greece					
November 12-16, 2012	"Demetallation of Ferrocene Boronic Acid Catalyzed by Gold Catalysts" at IKCOC-12 at Kyto, Japan					
January 20-23, 2013	"Esterification of fatty acid catalyzed by hydrothermally stable propylsulfonic acid-functionalized mesoporous silica SBA-15" at Euro-Asia Zeolite Conference at Macau, China					
May 21-23, 2013	"Surface Modification of Polycyclopentene- <i>co</i> -N-(4-aminophenyl)-5-norbornene-2,3-dicarboximide by Grafting with Polyaniline" at the 3 rd -Frontiers in Polymer Science at Sitges, Spain.					
July 14-19, 2013	"Ring-Opening Metathesis Polymerization of Cyclopentene and <i>N</i> -(4-Aminophenyl)-5-Norbornene-2,3-Dicarboximide and Surface Modification of Copolymer by Grafting Polymerization of Aniline" at 20 th International Symposium of Olefin Metathesis at Nara, Japan					

Unexpected Radical Polymerization of Methyl Methacrylate

Catalyzed by Cu(I)/Tripodal Ligand with Ferrocene Moieties

Atchariya Sunsin and Ekasith Somsook*

NANOCAST Laboratory, Center for Catalysis, Department of Chemistry and Center of Excellence for

Innovation in Chemistry, Faculty of Science, Mahidol University, 272 Thung Phaya Thai, Rama VI Rd.,

Ratchathewi, Bangkok 10400, Thailand

ABSTRACT

The polymerization of methyl methacrylate (MMA) catalyzed by CuBr/tris(2-(ferrocenyl

methylamino)ethyl)amine unexpectedly proceeded in the absence of alkyl halide. The growth of

molecular weight and the conversion were linearly dependent indicating the living character of radical

polymerization process. Reaction between CuBr and tris(2-(ferrocenyl methylamino)ethyl)amine

showed the formation of Cu(II) as evidenced from electron paramagnetic resonance (EPR) study.

Moreover, the radical trapping by (2,2,6,6-tetramethyl-piperidin-1-yl)oxyl (TEMPO) and the deuterated

labeling ligand in the presence of CuBr indicated that the polymerization proceeded via a radical

mechanism.

KEYWORDS: Ferrocene; Tripodal Ligand; Radical Polymerization

1

1. Introduction

$$\begin{array}{c} & & \text{Termination} \\ k_t & & \\ \hline Mt^n/Ligand + R-X & \underbrace{\frac{k_{act}}{k_{deact}}}_{\text{k_{deact}}} & R^{\bullet} + X\text{-Mt}^{n+1}/Ligand \\ & & \\ \hline Monomer & \end{array}$$

Scheme 1.

Atom transfer radical polymerization (ATRP) [1, 2] has become a powerful technique in many applications [3-5] for constructing functional polymers with well-defined composition, predictable topology, desired functionality, controlled molecular weight and narrow molecular weight distribution. As shown in Scheme 1, the general ATRP mechanism firstly proceeds by a halogen exchange between a lower oxidation state complex catalyst and an initiator (such as alkyl halide) to generate an active radical at appropriate low concentration and a higher oxidation state deactivated complex. The propagation of polymerization proceeds by sequential reactions of active radicals and other monomers to extend the chain length of active polymer radicals. The molecular weight and molecular weight distribution of polymers are controlled by the slow rate of termination, which is governed by the low concentration of radicals resulting from the equilibrium constant (K_{eq}) favoring the lower oxidation state complex. The living polymerization can be found in this polymerization due to most of polymer chains will be ended with a halide. It can react with the lower oxidation state complex to extend the polymer chain length endlessly as long as monomers are available in the reaction. Catalysts including metals and ligands are the key components to control the equilibrium constant (K_{eq}) . Similarly, different types of initiators showed an influence on the initiation of radicals in the ATRP rate constant [6]. Although alkyl halides are required in the halogen exchange step of the initiation mechanism, the alkyl halide-free ATRP of styrene and MMA were successfully carried out [7, 8] with an advantage to avoid any undesired property derived from alkyl halide.

Ferrocene is the most versatile molecule for tuning redox properties of materials in many applications [9-12]. It can be used as co-catalyst [13] or as additives [14-16] or as a moiety of monomer [17, 18] or as agents [19] in radical polymerization. In some cases, the rate of radical polymerization of MMA in the presence of zirconocene and benzoyl peroxide could be enhanced by the addition of ferrocene or ferrocene derivative [15, 16]. Herein, ferrocene moieties are proposed as redox mediators to enhance the rate of electron transfer process involved in the metal-catalyzed radical polymerization leading to the faster rate of controlled radical polymerization. Previously, ATRP of MMA catalyzed by CuBr/tripodal ligand containing ferrocene moieties was carried out to speed up the radical polymerization in a controlled manner with the addition of CuBr₂ [20, 21]. In the course of our studies on the ATRP of MMA catalyzed by CuBr/tripodal amine ligand containing ferrocene moieties, it turned out unexpectedly that the radical polymerization of MMA proceeded without the addition of alkyl halide. Here, the radical polymerization of MMA was investigated in the presence of Cu(I)/tripodal ligands with and without ferrocene moieties in the absence of alkyl halide as initiator.

2. Results and Discussion

Scheme 2.

As shown in Scheme 2, five ligands were synthesized for this study according to the modified previous reports [22, 23]. A mixture of tris(2-aminoethyl)amine (TREN) and ferrocene carboxaldehyde was stirred overnight in acetonitrile at room temperature yielding ligand 1. Then ligand 2 was synthesized by the reduction of ligand 1 in the presence of NaBH₄ in methanol. With benzaldehyde

and TREN as starting materials, ligand 3 and ligand 4 were synthesized sequentially with the similar procedures as ligand 1 and ligand 2, respectively. The deuterated ligand 5 was synthesized by the reduction of ligand 1 in the presence of NaBD₄. All products were characterized by ¹H NMR, ¹³C NMR and mass spectrometry. The polymerization of methyl methacrylate was carried out in a dried Schlenk flask under Ar atmosphere. CuBr and a selected ligand were added to the system. Then it was degassed and back-filled with argon gas for three times before adding monomer. Three cycles of freeze-pumpthaw were carried out before the reaction was immersed in an oil bath at a desired temperature. The polymerization started and the system was stirred for a period of time. To quench the polymerization, the system was cooled down in an ice bath and then THF was added. The obtained mixtures were filtered through an alumina column to remove the copper catalyst and then polymers were precipitated out in the excess amount of methanol. The yield of polymers were obtained after drying polymers under vacuum by gravimetry and the molecular weight (M_n) and the molecular weight distribution (PDI) were determined by Gel Permeation Chromatography (GPC). In addition, the yield percentages of polymers in kinetic studies were determined by ¹H NMR Spectroscopy calculated from the integral ratio of methoxy groups of polymers and monomers.

ATRP of MMA in the presence of catalyst containing ferrocene moieties was initially investigated to utilize ferrocene moieties as a redox mediator to enhance the catalytic activity by facilitating the rate of electron transfer in the polymerization. Cu(I) halide, a selected ligand, and an alkyl halide as an initiator are required for the ATRP of MMA. However, the bulk polymerization of MMA at 90 °C was started in the presence of CuBr and ligand 2 without the addition of an alkyl halide. As shown in Table 1, the polymerization of MMA could not proceed without the presence of both CuBr and ligand 2 (Table 1, entries 1-3). After the bulk polymerization of MMA in the presence of CuBr and ligand 2 proceeded for 1 hour, it turned out that the polymerization was not controlled resulting to the broad molecular weight distribution (Table 1, entry 4). However, the molecular weight distribution became narrower at shorter reaction time (Table 1, entry 5). Interestingly, the addition of alkyl halide resulted a broader molecular weight distribution (Table 1, entry 6).

Table 1. Bulk polymerization of MMA^a at 90 °C.

Entry	CuBr/Ligand 2 /MMA/I	Time (minutes)	%Yield	M _n (exp)	PDI
1	0/0/100/0	60	1	-	-
2	0/1/100/0	60	2	-	-
3	1/0/100/0	60	2	-	-
4	1/1/100/0	60	77	52900	2.28
5	1/1/100/0	20	65	25044	1.66
6 ^b	1/1/100/1	20	59	10158	1.87

^a Polymerization condition: [CuBr]:[Ligand 2]:[initiator]:[MMA] = 1:1:0:100 with [CuBr] = 0.0941 mol/dm³, [Ligand 2] = 0.0944 mol/dm³. ^b Polymerization condition: [CuBr]:[Ligand 2]:[initiator]:[MMA] = 1:1:1:100 with [CuBr] = 0.0932 mol/dm³, [Ligand 2] = 0.0931 mol/dm³ and [initiator] = 0.0931 mol/dm³.

Table 2. Bulk polymerization^a of MMA catalyzed by CuBr with various ligands at 90 °C.

Entry	Ligand	CuBr/Ligand/ MMA	Time (minutes)	%Yield	M _n (GPC)	DP _n ^c	PDI
1	1	1/1/100	300	22	299116	2988	2.37
2	2	1/1/100	60	77	52900	528	2.28
3	3	1/1/100	300	3	229401	2291	2.11
4	4	1/1/100	300	30	69252	692	2.06
5 ^b	5	1/1/100	30	55	43089	430	1.67

^a Polymerization condition: [CuBr]:[Ligand]:[initiator]:[MMA] = 1:1:0:100 with [CuBr] = 0.0941 mol/dm³, [Ligand 1] = 0.0930 mol/dm³, [Ligand 2] = 0.0944 mol/dm³, and [ligand 3] = [ligand 4] = 0.0929 mol/dm³. ^b Polymerization condition: [CuBr]:[Ligand 5]:[initiator]:[MMA] = 1:1:0:100 with [CuBr] = 0.0927 mol/dm³, [Ligand 2] = 0.0928 mol/dm³. ^c DP_n = MW of polymer/MW of monomer unit

Four different imine- and amine-typed ligands with and without ferrocene moieties were further investigated for the polymerization of MMA without the addition of alkyl halide as shown in Table 2. The rate of polymerization could be roughly determined by weighing the yields of polymers at a period of time. The ligand 3 system showed the lowest polymerization activity (Table 2, entry 3) while the ligands 1 and 4 showed comparable polymerization activities (Table 2, entries 1 and 4). Interestingly, the polymerization of MMA in the presence of ligand 2 showed the highest polymerization activity and the molecular weight distribution became broader at the longer reaction time as results from the slower rate of propagation and the faster rate of termination (Table 1, entry 5 and Table 2, entry 2). However, a high number of average molecular weight and degree of polymerization showed the faster rate of propagating than initiating process. The deuterated ligand 5 system showed a slightly lower activity than the ligand 2 system with comparable molecular weight distribution (Table 2, entry 5 and Table 1, entry 5). Accordingly, the comparison of molecular structures of ligands 1-4 implied that the H atoms at NH positions and ferrocenyl moieties might be involved in the catalytic process in the radical polymerization of MMA. This result is in agreement with the previous study recently [24]. Ferrocene and its derivative containing nitrogen atom were used to accelerate the efficiency of initial polymerization for controlled radical polymerization of MMA. Hence, a proposed mechanism of this radical polymerization is shown in Scheme 3, where I is a radical initiator, M is monomer and Fc is ferrocene moiety of copper complex. The radical polymerization of MMA for CuBr/Ligand 2 might be controlled by the through-space interactions between polymeryl radicals and metal complex containing ferrocene moieties leading to the lower rate of termination. This interaction may be weaker as the polymer chain became longer resulting to the broader molecular weight distribution at longer reaction time.

$$I \longrightarrow R'$$

$$R' + M \longrightarrow RM'$$

$$(+M)$$

$$k_p$$

$$\dot{M} \sim + Fc \longrightarrow [\sim M - \cdots - Fc]$$

$$(+M)$$

$$k_p$$

Scheme 3.

Table 3. Bulk polymerization^a of MMA catalyzed by CuBr/ligand 2 at various temperatures.

Entry	Cu/Ligand 2/MMA	Temperature(°C)	%Yield	M _n (GPC)	DP _n ^b	PDI
1	1/1/100	30	37	43203	432	2.05
2	1/1/100	60	71	46000	459	1.64
3	1/1/100	90	77	52900	528	2.28

^a Polymerization condition: [CuBr]:[Ligand **2**]:[initiator]:[MMA] = 1:1:0:100 with [CuBr] = 0.0941 mol/dm³, [Ligand **2**] = 0.0928 mol/dm³, reaction time 60 minutes. ^b DP_n = MW of polymer/MW of monomer unit

The effects of temperatures and halide counterions on the polymerization were also investigated. As shown in Table 3, the radical polymerization of MMA catalyzed by CuBr/ligand 2 proceeded successfully with 37% yield of polymer in the absence of alkyl halide at ambient temperature (Table 3, entry 1). As increasing temperature from 30° C to 60° C, a dramatic increasing of the reaction rate was observed with a better-controlled molecular weight distribution (Table 3, entry 2). However, the molecular weight distribution became broader as increasing temperature to 90 °C (Table 3, entry 3). To further investigations, the polymerization at 90 °C was chosen for our study because this temperature is commonly used for the polymerization of MMA.

Table 4. Bulk polymerization^a of MMA catalyzed by copper halide and ligand **2** at 90 °C.

Entry	Copper	Cu/L/MMA	Time	%Yield	M _n (GPC)	DP _n ^c	PDI
salt salt	Cu/L/MMA	(minutes)	/0 1 ICIU	M _n (Gr C)	DI n	I DI	
1	CuI	1/1/100	20	46	66014	659	2.74
2	CuBr	1/1/100	20	65	25044	250	1.66
3	CuCl	1/1/100	20	79	50582	505	2.31
4^{b}	$CuBr_2$	1/1/100	20	41	36128	361	1.65

^a Polymerization condition: [CuX]:[Ligand 2]:[initiator]:[MMA] = 1:1:0:100 with [CuCl] = [CuBr] = [CuI] = 0.0940 mol/dm³, [Ligand 2] = 0.0944 mol/dm³. ^b Polymerization condition: [CuBr₂]:[Ligand 2]:[initiator]:[MMA] = 1:1:0:100 with [CuBr₂] = 0.0929 mol/dm³, [Ligand 2] = 0.0930 mol/dm³. ^c DP_n = MW of polymer/MW of monomer unit.

The bulk polymerization of MMA catalyzed by copper halide and ligand 2 is shown in Table 4. For the Cu(I) systems, the chloride system exhibited the fastest rate of polymerization with 79% yield, PDI = 2.31 while the iodide system showed slowest polymerization rate with 46% yield, PDI = 2.74. High values of both number average molecular weight (M_n) and degree of polymerization (DP) indicated that both catalyst systems had a low power of catalysis with a poor generation of initial radicals and a low level of control the polymerization. Interestingly, while the bromide system showed a comparable rate of polymerization to the chloride system, the molecular weight distribution was narrower for the bromide system. The oxidation state of copper also influenced the rate of polymerization. The CuBr₂ system showed the same molecular weight distribution to the CuBr system but the rate of polymerization became sluggish for Cu(II) system. Nevertheless, the CuBr/ligand 2 was the most effective catalyst with the low degree of polymerization compared to other systems.

The addition of Ag(OTf) to the polymerization transformed ferrocene moieties in a complex to ferricinium moieties [25, 26]. A separate experiment starting by mixing ligand 2 with MMA, then Ag(OTf) was added to the mixture with a color change to dark gray-green color. It was stirred for 15 minutes before adding CuBr. Then the reaction was carried out at 90 °C for 1 hour. It turned out that

only 2% polymer yield was obtained. Similarly, only trace of polymer was obtained if mixing CuBr with ligand 2 and MMA at the beginning, then Ag(OTf) was added to the mixture and the reaction was allowed to be carried out at 90 °C for 1 hour. Our results showed that ferricinium moieties were inhibitors for the radical generation and/or CuBr/Ligand 2 complex was destabilized with the reaction with Ag(OTf). Therefore, ferricinium may not be involved in the polymerization of MMA in the presence of CuBr/Ligand 2.

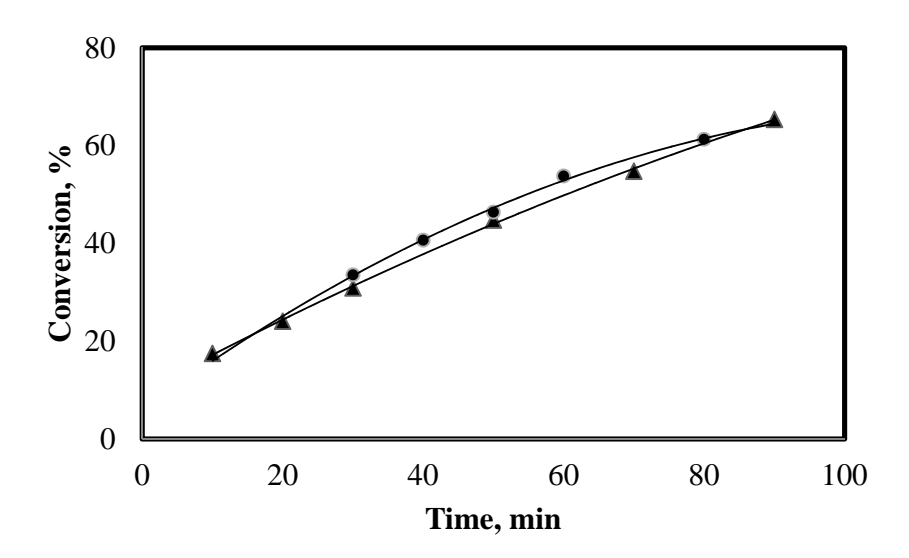


Figure 1. The kinetic plot of polymerization of MMA catalyzed by CuBr/ligand **2** in 50% v/v toluene: [Monomer]:[Catalyst] is 100:1 (\bullet) with [CuBr] = 0.0471 mol/dm³ and [Ligand **2**] = 0.0471 mol/dm³ and [Monomer]:[Catalyst] is 200:1 (\blacktriangle) with [CuBr] = 0.0236 mol/dm³ and [Ligand **2**] = 0.0235 mol/dm³.

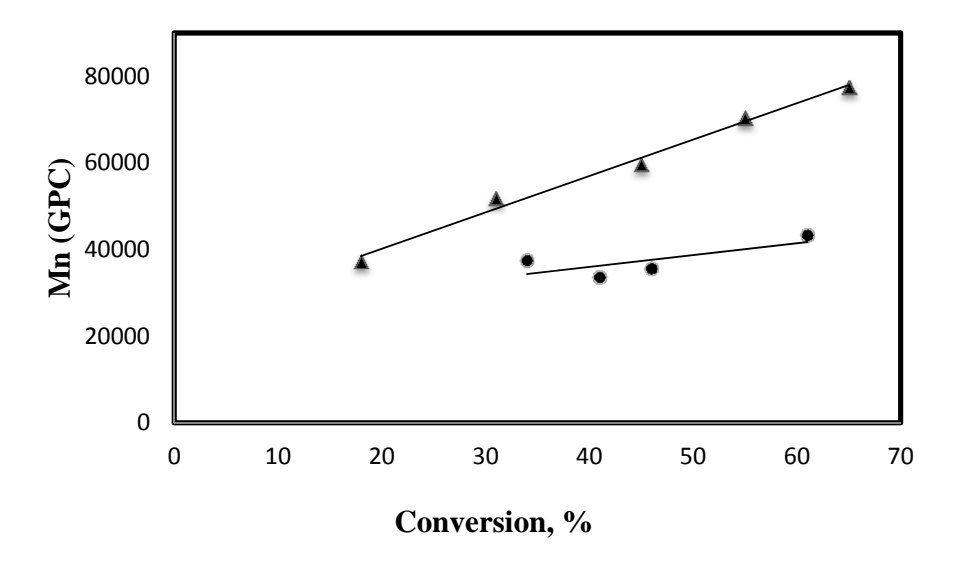


Figure 2. Molecular evolution of polymer products from the polymerization of MMA catalyzed by CuBr/ligand **2** in 50% v/v toluene: [Monomer]:[Catalyst] is 100:1 (\bullet) with [CuBr] = 0.0471 mol/dm³ and [Ligand **2**] = 0.0471 mol/dm³ and [Monomer]:[Catalyst] is 200:1 (\blacktriangle) with [CuBr] = 0.0236 mol/dm³ and [Ligand **2**] = 0.0235 mol/dm³.

The effect of molar ratio of monomer to catalyst on the polymerization rate was also investigated. The kinetic study showed that there was no significant difference of the polymerization rate for both molar ratios at 100:1 and 200:1 as shown in Figure 1. This confirmed that the rate of polymerization was independent of the monomer concentration. Also, the radical initiator may not be originated from the monomer. The evolution of molecular weight showed a linear function with the monomer conversion indicating the living character of the radical polymer chain as shown in Figure 2. However, the broadening of molecular weight distribution (in range of 1.59-1.99 and 1.72-1.92 for monomer to catalyst as 100:1 and 200:1, respectively) indicated a high termination process in the system.

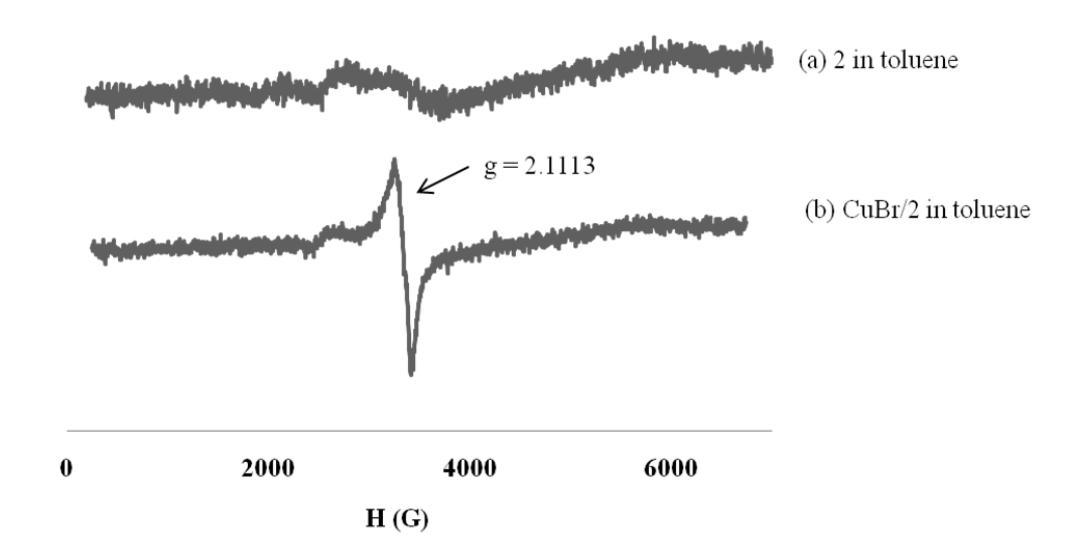


Figure 3. EPR spectra of (a) fresh ligand 2, (b) the mixture of CuBr and ligand 2 in toluene.

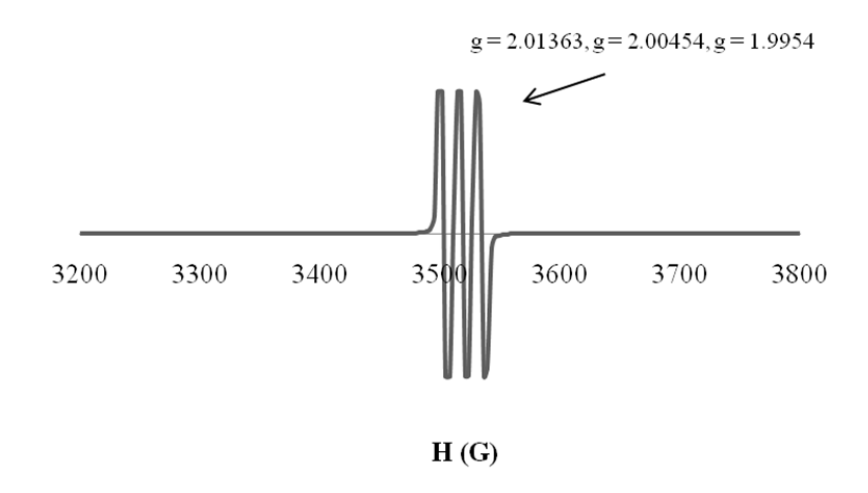


Figure 4. EPR spectrum of ligand 2 kept for 50 days.

As shown in Figure 3, electron paramagnetic resonance (EPR) spectra of fresh ligand 2 and the mixture of CuBr and ligand 2 were collected to investigate the role of catalyst in the polymerization. Fresh ligand 2 showed a EPR silent signal while the characteristic of unsymmetrical EPR signal of Cu(II) was observed for the mixture of CuBr and ligand 2 in toluene. Moreover, ligand 2 kept for a long time showed a triplet EPR signal with a ratio of 1:1:1 and a hyperfine splitting constant of 1.59 mT. This indicated that ligand 2 could generate radicals by N-H homolytic cleavage. The previous report

[27] showed that NH proton of Cu(II)/ligand 4 could be deprotonated and oxidized by oxygen in air leading to Cu(I)-imine complex. However, the radical derived from ligand 2 was generated by the homolytic cleavage of N-H bond as accelerated by a through-space interaction between ferrocene moieties and nitrogen donor atom and it became more pronounced when ligand 2 was complexed to Cu(I) leading to Cu(I)-radical as shown in Scheme 4. Cu(II) complex was then formed as observed by EPR spectroscopy. The polymerization may be initiated by the homolytic cleavage of N-H bond in the Cu(I) complex and transfer hydrogen to react with a monomer to generate a monomer radical in which polymer chains were formed by the propagation from this radical with other monomers. It was questionable whether the ATRP process also proceeded during the radical polymerization. Attempting to detect the chain end of halogen groups was unsuccessful.

Scheme 4. A proposed mechanism involving the dissociation of H from Cu(I) complex resulting to the formation of Cu(II) complex stabilized by ferrocene moieties.

Scheme 5. A mechanism model of radical trapping between TEMPO and the dissociated deuterium radical from Cu(I) complex.

According to the previously mentioned hypotheses, the deuterium labeled ligand 5 was synthesized to determine the species involving in the system. This experiment was modified from the activation rate constant measurement in ATRP [28] by using (2,2,6,6-tetramethyl-piperidin-1-yl)oxyl (TEMPO) as a radical scavenger as shown in Scheme 5 and then the trapped species were determined by Electrospray Ionization (ESI) mass spectrometry. First, the radical trapping experiment was carried out by the addition of TEMPO to quench the bulk polymerization of MMA catalyzed by CuBr/ligand 2 at 90 °C. The result showed that the polymerization process was terminated with the addition of TEMPO giving no polymer even though the reaction was carried out at 90 °C for 1 hour. In addition, the mass spectrum of the residue after the removal of catalyst showed m/z at 257.13, 297.26 and 491.28. The m/z at 257.13 was assigned to the trapped product between TEMPO and MMA. In another experiment between CuBr, Ligand 5, and TEMPO in a ratio of 1:1:5 in dried acetonitrile, it was found

by positive ion ESI-mass spectrometry with peaks m/z at 885.05 and 887.05 assigned to Cu(II)-imine complex and m/z at 158.16 and 159.16 assigned to [TEMPOH-H]⁺ as shown in Scheme 5. The characteristic peaks of TEMPO in acetonitrile on positive ion ESI mass spectrum were found at m/z 156, 157, and 158 [29]. It was unsuccessful to obtain TEMPOD. Therefore, the first radical species at the initial stage of polymerization of MMA in the presence of CuBr/Ligand 2 might be involved in the release of hydrogen from the ligand and then monomers radicals were generated from the reaction with hydrogen transferred in the system and then it was propagated with other monomers as the polymerization was controlled by the interaction between polymeryl radicals and ferrocene moieties of CuBr/Ligand 2.

3. Conclusion

The CuBr/ligand 2 catalyst showed a successful polymerization of MMA without the addition of alkyl halide. A linear relationship between an average molecular weight and conversion indicated a characteristic of living radical polymerization. EPR spectroscopy, the radical trapping by TEMPO and the deuterated labeling experiments showed that the polymerization proceeded via a radical mechanism initiated by a radical generated by a homolytic cleavage of N-H bonds of Cu(I) complex and controlled by the interaction between polymeryl radicals and ferrocenyl complex. This interaction became weaker as the growing of polymer chains resulting to the broader molecular weight distribution.

Acknowledgements

The financial supports by the Thailand Research Fund-the Office of the Higher Education (RMU5380043), Center of Excellence for Innovation in Chemistry (PERCH-CIC), and the Office of the Higher Education Commission-Mahidol University under the National Research University Initiative are acknowledged.

References

- [1] K. Matyjaszewski, Macromolecules, 45 (2012) 4015-4039.
- [2] M. Ouchi, T. Terashima, M. Sawamoto, Chem. Rev., 109 (2009) 4963-5050.

- [3] D.S.H. Chu, J.G. Schellinger, J.L. Shi, A.J. Convertine, P.S. Stayton, S.H. Pun, Acc. Chem. Res., 45 (2012) 1089-1099.
- [4] J.D. Cushen, I. Otsuka, C.M. Bates, S. Halila, S. Fort, C. Rochas, J.A. Easley, E.L. Rausch, A. Thio, R. Borsali, C.G. Willson, C.J. Ellison, ACS Nano, 6 (2012) 3424-3433.
- [5] A.M. Telford, L. Meagher, V. Glattauer, T.R. Gengenbach, C.D. Easton, C. Neto, Biomacromolecules, 13 (2012) 2989-2996.
- [6] K. Matyjaszewski, H.J. Paik, P. Zhou, S.J. Diamanti, Macromolecules, 34 (2001) 5125-5131.
- [7] Z.P. Cheng, X.L. Zhu, N.C. Zhou, J.M. Lu, J. Appl. Polym. Sci., 90 (2003) 1532-1538.
- [8] Y.Q. Xu, Q.F. Xu, J.M. Lu, X.W. Xia, L.H. Wang, Eur. Polym. J., 43 (2007) 2028-2034.
- [9] T. Daeneke, A.J. Mozer, T.H. Kwon, N.W. Duffy, A.B. Holmes, U. Bach, L. Spiccia, Energy Environ. Sci., 5 (2012) 7090-7099.
- [10] C.M. Casado, I. Cuadrado, M. Moran, B. Alonso, B. Garcia, B. Gonzalez, J. Losada, Coord. Chem. Rev., 185-6 (1999) 53-79.
- [11] L.B. Deng, L. Wang, H.J. Yu, X.C. Dong, J. Huo, Des. Monomers Polym., 10 (2007) 131-143.
- [12] Y.J. Ma, W.F. Dong, M.A. Hempenius, H. Mohwald, G.J. Vancso, Nat. Mater., 5 (2006) 724-729.
- [13] K. Fujimura, M. Ouchi, M. Sawamoto, ACS Macro. Lett., 1 (2012) 321-323.
- [14] Y.I. Puzin, R.K. Yumagulova, V.A. Kraikin, Eur. Polym. J., 37 (2001) 1801-1812.
- [15] Y.B. Monakov, R.M. Islamova, A.K. Frizen, O.I. Golovochesova, S.V. Nazarova, Mendeleev Commun., 22 (2012) 55-55.
- [16] Y.B. Monakov, Y.I. Puzin, A.V. Zaikina, E.I. Yarmukhamedova, A.A. Fatykhov, G.E. Zaikov, J. Appl. Polym. Sci., 103 (2007) 724-727.
- [17] C. Herfurth, D. Voll, J. Buller, J. Weiss, C. Barner-Kowollik, A. Laschewsky, J. Polym. Sci. Polym. Chem., 50 (2012) 108-118.
- [18] N.N. Sigaeva, A.K. Friesen, I.I. Nasibullin, N.L. Ermolaev, S.V. Kolesov, Polym. Sci. Ser. B+, 54 (2012) 197-204.
- [19] N.C. Zhou, Z.B. Zhang, J. Zhu, Z.P. Cheng, X.L. Zhu, Macromolecules, 42 (2009) 3898-3905.
- [20] A. Sunsin, N. Wisutsri, S. Suriyarak, R. Teanchai, S. Jindabot, L. Chaicharoenwimolkul, E. Somsook, J. Appl. Polym. Sci., 113 (2009) 3766-3773.
- [21] P. Sangtrirutnugul, P. Maisopa, L. Chaicharoenwimolkul, A. Sunsin, E. Somsook, V. Reutrakul, J. Appl. Polym. Sci. DOI: 10.1002/app.37596.
- [22] E.C. Brown, B. Johnson, S. Palavicini, B.E. Kucera, L. Casella, W.B. Tolman, Dalton Trans., (2007) 3035-3042.
- [23] M. Heitzmann, J.C. Moutet, J. Pecaut, O. Reynes, G. Royal, E. Saint-Aman, G. Serratrice, Eur. J. Inorg. Chem., (2003) 4262-4262.
- [24] R.M. Islamova, Y.B. Monakov, Metal-Complex Compounds as Components of Initiating Systems for the Controlled Radical Polymerization of Vinyl Monomers, Polym. Sci. Ser. C+, 53 (2011) 27-34.
- [25] C.K.A. Gregson, V.C. Gibson, N.J. Long, E.L. Marshall, P.J. Oxford, A.J.P. White, J. Am. Chem. Soc., 128 (2006) 7410-7411.
- [26] E.M. Broderick, N. Guo, C.S. Vogel, C.L. Xu, J. Sutter, J.T. Miller, K. Meyer, P. Mehrkhodavandi, P.L. Diaconescu, J. Am. Chem. Soc., 133 (2011) 9278-9281.
- [27] M. Schatz, M. Becker, O. Walter, G. Liehr, S. Schindler, Inorg. Chim. Acta, 324 (2001) 173-179.
- [28] W. Tang, K. Matyjaszewski, Macromolecules, 39 (2006) 4953-4959.
- [29] X. Zhang, H.Y. Wang, Y.L. Guo, Rapid Commun. Mass Spectrom, 20 (2006) 1877-1882.

Atom Transfer Radical Polymerization Catalyzed by Cu/Bidentate Ligand with Ferrocene Moieties

Udomchai Tewasekson and Ekasith Somsook*

NANOCAST Laboratory, Center for Catalysis, Department of Chemistry and Center for Innovation in Chemistry, Faculty of Science, Mahidol University, 272 Rama VI Rd., Thung Phaya Thai, Ratchathewi, Bangkok 10400, Thailand.

E-mail address: ekasith.som@mahidol.ac.th Tel: +662-201-5123 Fax: +662-354-7151

* To whom correspondence should be addressed.

Abstract:

Atom Transfer Radical Polymerization (ATRP) is one of "controlled/living" radical

polymerization in which polymer can be yielded with controlled composition, morphology and low

molecular weight distribution (PDI). In this work, catalysts with ferrocene moiety are proposed to be

used to enhance the catalytic activities of ATRP of methyl methacrylate (MMA). Copper(II)

iminopyridine complexes were prepared and used in Activator Generated by Electron Transfer

(AGET) ATRP of MMA by using ascorbic acid as a reducing agent. The comparable PDIs (>1.5) in

both bulk and solution conditions were obtained. In addition, the polymerization can be started

without the addition of reducing agents. Kinetic studies revealed a slow initiation behavior which an

induction period was required to start the reaction. These results indicated that ferrocene moiety as a

redox switchable molecule may improve an electron transfer process of the catalyst in the

polymerization.

Keywords: ATRP, ferrocene

Introduction

Atom Transfer Radical Polymerization (ATRP) is one of "controlled/living" radical polymerization in which polymers can be yield with controlled composition, morphology and low molecular weight distribution (PDI). Catalysts plays an important role in this process by the control of electron and halide transportation. Basically, ATRP catalysts are air-sensitive resulting to a special set-up for a polymerization. Recently, several air-stable catalysts have been developed for ATRP such as Activator Generated by Electron Transfer (AGET) in which a reducing agent is used to reduce an air-stable precatalyst to an active catalyst. Ferrocene is an organometallic molecule used in many catalytic applications because its stability, biocompettibility and redox properties. In this work, ferrocene moiety was incorporated into bidentate ligands and then complexes with these ligands were catalysts for ATRP of MMA and ascorbic acid was used as a reducing agent in AGET ATRP.



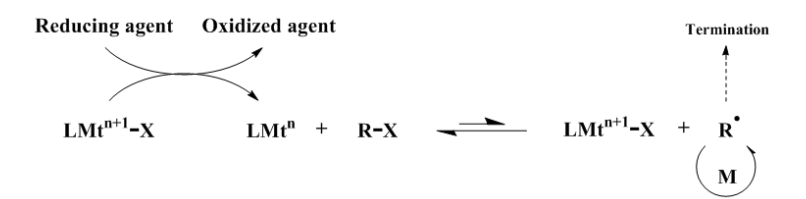


Fig 1. General scheme of normal ATRP (upper) and AGET ATRP (lower)

Experimental

General procedure for AGET ATRP was performed under Ar atmosphere. A dry Schlenk flask which sealed with septa was switched between vacuumed and Ar for 5 min., 3 times. The catalyst and ascorbic acid were added to the flask and then seal with stopper and switched between vacuum and Ar for 5 min., 3 times once again. MMA was injected by syringe which purged by Ar. The mixture was removed O_2 by freeze-pump-thaw technique 10min, 3 times. The solution was stirred at room temperature for 5 min. and preheats at 90° C in oil bath for more 5 min. While stirring at polymerization temperature, ethyl 2-bromoisobutylrate was injected to the mixture by changing stopper to septa. Then, the flask was sealed with stopper and allowed polymerization to proceed. After desire time, the reaction was quenched by THF and cooled to room temperature. The residues were removed by alumina neutral column. The solution was concentrated by rotary evaporator and then washed with methanol in an excess amount. The polymer product will be obtained and dry in vacuum to calculate % yield. The M_n and PDI were characterized by Gel permeation Chromatography (GPC).

For kinetics study, A dry schlenk flask which sealed with septa was switched between vacuumed and Ar for 5 min., 3 times. The catalyst was added to the flask and then seal with stopper and switch between vacuumed and Ar for 5 min., 3 times once again. MMA was added by syringe which purge by Ar. The mixture was removed O₂ and H₂O by freeze-pump-thaw technique 10min, 3 times. By changing stopper to septa, Toluene was inject into the reaction and then stirs at room temperature for 5 min. and preheats at 90°C in oil bath for more 5 min. While stirring at polymerization temperature, ethyl 2-bromoisobutylrate was inject to the mixture to start the reaction. The solution was sampling every 4h. until 24h. The sample was divided into 2 parts; First part was added to methanol in an excess amount to precipitated polymer product for PDI investigation. The second part was added into chloroform-d to prepared NMR sample for %yield investigation.

Results and Discussion

Complexes of iminopyridine ligand were synthesized by addition of anhydrous Na_2SO_4 in to the solution of 1-pyridinecarbaldehyde and aniline derivative in CH_2Cl_2 . The mixtures were stirred at

room temperature for 3hours. The solid was filter off and $CuBr_2$ was added to the solution then continued stirring to 24 hours. The mixture was filtered to remove some residue and dry under vacuum.

Fig 2. Expected complexes (1) CuBr₂-dine2A (2) CuBr₂-dine2N (3) CuBr₂-dine2T (4) CuBr₂-dine2M

 $\label{eq:TABLE 1} \textbf{Polymerization of MMA (MMA = methyl methacrylate) in bulk}$

Entry	MMA/Catalyst/EBIB/Ascorbic acid	Time (h.)	% yield	M_n (theo) ^a	M_n (GPC)	M_w/M_n
1 ^b	100:1:1:0.5	5	9	-	-	-
2 ^b	100:1:1:0.5	24	7	-	-	-
3 ^c	100:1:1:0.5	5	10	-	-	-
4 ^c	100:1:1:0.5	20	8	-	-	-
5 ^d	100:1:1:0.5	5	10	-	-	-
6^{d}	100:1:1:0.5	20	10	-	-	-
7 ^e	100:1:1:0.5	5	74	7,707	19,549	1.43
8 ^b	100:1:1:0	20	9	-	-	-
9 ^d	100:1:1:0	20	10	-	-	-

initiated by EBIB (EBIB = ethyl 2-bromoisobuthylrate) at 90 $^{\rm o}$ C.

10 ^e	100:1:1:0	5	85	8,823	20294	1.55
11 ^e	100:1:0:0	5	9	-	-	-
$12^{e,f}$	100:1:1:0	5	76	7,927	32,404	1.46
13 ^{e,g}	100:1:1:0	5	34	3,654	26,153	1.39

^a M_n (theo) = [([Monomer]₀/[Initiator]₀) X Conversion X MW_{monomer}] + MW_{initiator}, where MW_{monomer} is the monomer molecular weight and MW_{initiator} is the initiator molecular weight.

Polymerization by Complexes (4) yield product about 75% yields in 5h. while the others yield only 10 % since 5-20h. PDI of the product was 1.43 which is relatively low (less than 1.5) but $M_{n,GPC}$ is 2 times higher than $M_{n,theo}$ represent the faster rate of propagation over initiation. This indicated that ferrocene moiety can enhance catalytic activity of the catalyst without losing the controllability. There are report about outer sphere electron transfer (OSET) between catalyst and MMA result in reduction of catalyst without addition of any additive. Thus, the experiments without ascorbic acid were performed. The result shows that the reaction can be preceded by complex 4 only correspond to AGET results (Teble 1, entry 8-10). This indicates that OSET and ATRP were promoted by a present of ferrocene moiety. In the absent of initiator, polymerization cannot be take placed show that radical cannot be generated by complex with ferrocene moiety(Table 1, entry 11). Limitation of this study lies on disturbance of the substrate of catalysts which were synthesized *in situ* and used without purification. Thus, 5 mole % of *m*-ferrocenyl aniline and pyridine 2-carboxaldehyde were added to the reaction (tale 1, entry 12, 13) to investigate the effect of impurities. In the present of *m*-ferrocenyl aniline, the result wasn't different from the early experiment while the present of pyrrole 2-carboxaldehyde showed the decreasing of %yield. PDI of both product still around 1.4 which exhibit

^b Catalyst = $CuBr_2$ -dine2A (1)

 $^{^{}c}$ Catalyst = CuBr₂-dine2N (2)

^d Catalyst = $CuBr_2$ -dine2T (3)

 $^{^{}e}$ Catalyst = CuBr₂-dine2M (4)

f Addition of 5% mol m-ferrocenylaniline with respect to CuBr₂

g Addition of 5% mol pyridine 2-carboxaldehyde with respect to CuBr₂

the controllability of process. This may determine that the catalytic activity of pure catalysts was possibly deteriorated by impurities. Finally, Polymerization of methyl methacrylate by complex (4) in toluene was performed for study the kinetics of reaction. The samples were sampling every 4 hours until 24 h (table 2, entry 1-6). The induction period occur at first 4h. result in the absent of polymer product. After that, the product was present and increasing respect to time. Figure 3 (a) and (b) showed the parabolic and invert parabolic curve which can be indicated to a slow initiation corresponded to the result from bulk condition. The PDI values were slightly increased with time represent the losing of controllability which was the character of general radical polymerization.

In the conclusion, Ferrocene moiety can enhance catalytic activity of ATRP's catalyst without losing controllability in both bulk and solution condition. Moreover, this system can be initiated without reducing agent due to the outer sphere electron transfer process which was promoted via intramolecular electron transfer between Cu and ferrocene as well.

TABLE 2 $\label{eq:GAMA} GAMA\ ATRPof\ MMA\ (MMA=methyl\ methacrylate)\ in\ toluene\ solution\ (50\ \%\ v/v)$ initiated by EBIB (EBIB = ethyl\ 2-bromoisobuthylrate)\ at\ 90\ ^{\circ}C.

Entry ^b	MMA/Catalyst/EBIB/Ascorbic acid	Time (h.)	% yield	M_n (theo) ^a	M _n (GPC)	M_w/M_n
1	100:1:1:0	4	0	-	-	-
2	100:1:1:0	8	17	1,903	13,512	1.32
3	100:1:1:0	12	41	4,316	22,528	1.33
4	100:1:1:0	16	64	6,627	23,605	1.46
5	100:1:1:0	20	79	8,135	24,553	1.49
6	100:1:1:0	24	86	8,839	25,604	1.49

^a M_n (theo) = [([Monomer]₀/[Initiator]₀) X Conversion X MW_{monomer}] + MW_{initiator}, where MW_{monomer} is the monomer molecular weight and MW_{initiator} is the initiator molecular weight.

^b Catalyst = CuBr₂-dine2M (4)

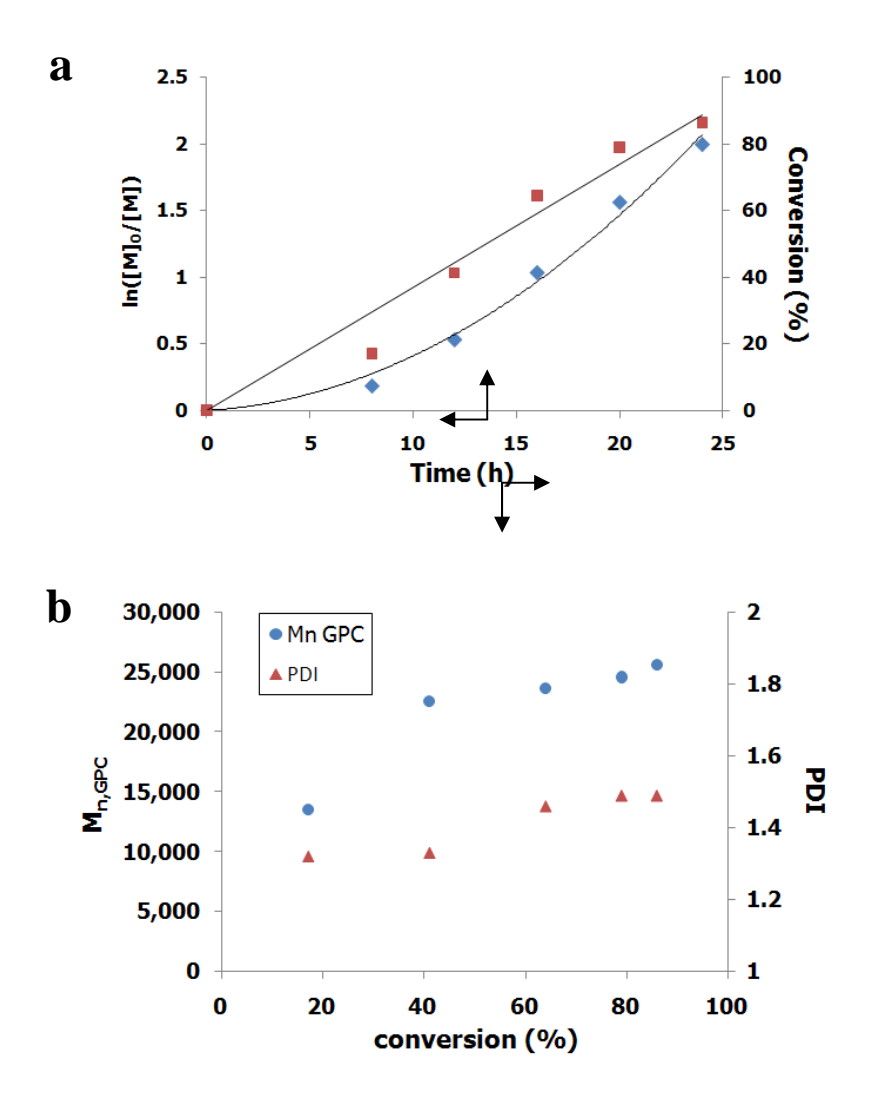


Fig. 1. $ln([M]_0/[M])$ and conversion as a function of time (a) and average-number molecular weight $(M_{n,GPC})$ and poly dispersity index (PDI) versus the conversion (b) for polymerization of MMA . Polymerization condition: $[MMA]/[EBIB]/CuBr_2$ -dine2M = 100/1/1; [MMA] = 4.6 M; temperature $= 90^{\circ}C$; solvent = toluene 50% v/v.

3.1 AGET ATRP of methyl methacrylate

To investigate the electronic effect of ferrocene moiety, the steric effect has to be avoid by using bidentate ligand even thought it's a poor ligand for ATRP. –H, –CH₃ and –NO₂ substituent groups as a representative of hydrogen substituent, electron donating and electron donating group were compared the result with ferrocenyl substituent group. Table 1, entry 1-7 showed the results from AGET ATRP by using complexes of 4 ligands. Polymerization by Complexes (4) yield product about 75% yields in 5h. while the others yield only 10 % since 5 – 20h. PDI of the product was 1.43 which is relatively low (less than 1.5) but $M_{n,GPC}$ is 2 times higher than $M_{n,theo}$ represent the faster rate of propagation over initiation. This indicated that ferrocene moiety can enhance catalytic activity of the catalyst without losing the controllability.

3.2 Polymerization of methyl methacrylate without the reducing agent and initiator

To verify function of complex (4), polymerizations without reducing agent and initiator were performed separately. In the absent of ascorbic acid, polymerization still can be proceeded with slightly increasing of % yield and PDI (Table 1, entry 10) while the polymerization without initiator cannot be take placed (Table 1, entry 11). These results were similar to the experiment of Matyjaszewski et al. in 2003 and Schubert et al. in 2007. The plausible mechanism was outer sphere electron transfer (OSET) which was promoted via intramolecular electron transfer between Cu and ferrocene. Slow initiation was appeared from this phenomena as well.

3.3 Effect of impurities.

The experiments can be disturbed by the substrate of catalysts which were synthesized *in situ* and used without purification. Thus, 5 mole % of *m*-ferrocenyl aniline and pyridine 2-carboxaldehyde were added to the reaction (table 1, entry 12, 13) to investigate the effect of impurities. In the present of *m*-ferrocenyl aniline, the result wasn't different from the early experiment while the present of pyrrole 2-carboxaldehyde showed the decreasing of %yield. PDI of both product still around 1.4 which exhibit the controllability of process. This may assure that the catalytic activity of catalyst in this work was possibly minimized.

3.4 Kinetics study

Polymerization of methyl methacrylate by complex (4) in toluene was performed for study the kinetics of reaction. The samples were sampling every 4 hours until 24 h (table 2, entry 1-6). The induction period occur at first 4h. result in the absent of polymer product. After that, the product was present and increasing respect to time. Figure 1(a) and (b) showed the parabolic and invert parabolic curve which can be indicated to a slow initiation corresponded to the result from bulk condition. The PDI values were slightly increased with time represent the losing of controllability which was the character of general radical polymerization.

To investigate the electronic effect of ferrocene moiety, the steric effect has to be avoid by using bidentate ligand even thought it's a poor ligand for ATRP. -H, -CH₃ and -NO₂ substituent groups as a representative of hydrogen substituent, electron donating and electron donating group were compared the result with ferrocenyl substituent group. Table 1, entry 1-7 showed the results from AGET ATRP by using complexes of 4 ligands. Polymerization by Complexes (4) yield product about 75% yields in 5h. while the others yield only 10 % since 5 – 20h. PDI of the product was 1.43 which is relatively low (less than 1.5) but $M_{n,GPC}$ is 2 times higher than $M_{n,theo}$ represent the faster rate of propagation over initiation. This indicated that ferrocene moiety can enhance catalytic activity of the catalyst without losing the controllability. GAMA ATRP was performed to verify the appearance of outer sphere electron transfer (OSET) between catalyst and MMA. The result shows that the reaction can be proceeded by complex 4 only correspond to AGET results (Teble 1, entry 8-10). This indicates that OSET and ATRP were promoted by a present of ferrocene moiety. In the absent of initiator, polymerization cannot be take placed show that radical cannot be generated by complex with ferrocene moiety(Table 1, entry 11). Limitation of this study lies on disturbance of the substrate of catalysts which were synthesized in situ and used without purification. Thus, 5 mole % of mferrocenyl aniline and pyridine 2-carboxaldehyde were added to the reaction (tale 1, entry 12, 13) to investigate the effect of impurities. In the present of m-ferrocenyl aniline, the result wasn't different from the early experiment while the present of pyrrole 2-carboxaldehyde showed the decreasing of % yield. PDI of both product still around 1.4 which exhibit the controllability of process. This may assure that the catalytic activity of catalyst in this work was possibly minimized. Finally, Polymerization of methyl methacrylate by complex (4) in toluene was performed for study the kinetics of reaction. The samples were sampling every 4 hours until 24 h (table 2, entry 1-6). The induction period occur at first 4h. result in the absent of polymer product. After that, the product was present and increasing respect to time. Figure 1(a) and (b) showed the parabolic and invert parabolic curve which can be indicated to a slow initiation corresponded to the result from bulk condition. The PDI values were slightly increased with time represent the losing of controllability which was the character of general radical polymerization.

4. Conclusion

Ferrocene moiety can enhance catalytic activity of ATRP's catalyst without loosing controllability in both bulk and solution condition. Moreover, this system can be initiated without reducing agent due to the outer sphere electron transfer process which was promoted via intramolecular electron transfer between Cu and ferrocene as well.

Effect of Ferrocene Substituents and Ferricinium Additive on the Properties of Polyaniline Derivatives and Catalytic Activities of Palladium-Doped Poly(*m*-ferrocenylaniline)-catalyzed Suzuki-Miyaura Cross-coupling Reactions

Laksamee Chaicharoenwimolkul, ^{1,2} Sanoe Chairam, ³ Montree Namkajorn, ¹ Achjana Khamthip, ¹ Choavarit Kamonsatikul, ¹ Udomchai Tewasekson, ¹ Sudarat Jindabot, ¹ Weeraphat Pon-On, ¹ Ekasith Somsook ¹*

¹NANOCAST Laboratory, Center for Catalysis, Department of Chemistry and Center for Innovation in Chemistry, Faculty of Science, Mahidol University, 272 Rama VI Rd., Thung Phaya Thai, Ratchathewi, Bangkok 10400, Thailand.

²School of Chemistry, Faculty of Science and Technology, Suratthani Rajabhat University, 272 Moo 9, Surat-Nasan Rd., Khuntale, Muang, Surat Thani 84100, Thailand.

³Department of Chemistry and Center for Innovation in Chemistry, Faculty of Science, Ubon Ratchathani University, Warinchamrap, Ubon Ratchathani 34190, Thailand.

E-mail address: ekasith.som@mahidol.ac.th Tel: +662-201-5123 Fax: +662-354-7151

^{*} To whom correspondence should be addressed.

ABSTRACT

Poly(aniline-*co-m*-ferrocenylaniline) and ferricinium-doped poly(aniline-*co-m*-

ferrocenylaniline) were synthesized by a conventional chemical oxidative polymerization,

then characterized by spectroscopic techniques and quantitative analyzes. Increasing of the

percentages of m-ferrocenylaniline in the copolymers resulted to a blue shift of UV-Vis

absorption spectra. Broader EPR spectra indicated the loss of conjugation and crystallinity of

copolymers. ¹H NMR spectra confirmed the presence of ferrocene moieties and ferricinium

in the polymers. The CV measurements showed that the electron withdrawing power of

ferrocene moieties could lead to the decreasing of electron delocalization on the polymer

main chain. The VSM results showed that as-prepared copolymers were soft magnetic

materials with very low magnetization. Pd-doped poly(m-ferrocenylaniline) as catalysts were

utilized in the Suzuki-Miyaura cross-coupling reactions to improve the catalytic activities.

KEYWORDS: Polyaniline derivatives; *m*-ferrocenylaniline; Ferricinium; Suzuki-Miyaura

cross-coupling.

Introduction

It is of special interest to investigate hybrid nanocomposites based on organic polymers which can be fabricated with various inorganic nanoparticles to create nanocatalysts with improvements in their properties for catalysis. In addition to the size and shape of nanocatalysts, it is apparent that some molecular factors such as the surface composition, charge transfer and oxidation state of the stabilizing ligand layers can be used to control the catalytic activity and selectivity of nanocatalysts high which can be chemically tuned with the redox property of appropriate ligands or polymers. Polyaniline is currently an excellent example of the most widely studied conducting polymers which can be synthesized by the oxidative polymerization of aniline in an aqueous acid solution with ease, either by using an electrochemical method or a chemical oxidant polymerization. In order to modify the properties of polymers, substituted polyanilines can be made by adding various functional groups to the backbone of the polymers or incorporating external dopants binding to the polymer backbone.

The Suzuki-Miyaura cross-coupling reaction of aryl halides with arylboronic acids is a fundamental transformation in modern organic synthesis and offers a powerful method for the aryl-aryl formation. Palladium complexes and nanoparticles are one of the most useful catalysts for carbon-carbon cross-coupling reactions. Recently, conjugated conductive polyaniline used as a supporter for palladium nanoparticles (PdNPs) has been reported as excellent catalysts in the cross-coupling reactions. A number of studies investigated ligands containing ferrocene covalently bonded for the metal-assisted cross-coupling reactions of aryl halides with arylboronic acids. As part of our efforts to synthesize a novel conjugated polymer, herein polyanilines based on the redox-active ferrocene moiety extended on the polymer backbone were synthesized, and their properties were investigated to improve the catalytic activities. The aims of this work were therefore to

prepare and characterize poly(aniline-*co-m*-ferrocenylaniline)(s) and ferricinium-doped poly(aniline-*co-m*-ferrocenylaniline)(s), and investigate the Suzuki-Miyaura cross-coupling activities catalyzed by the nanocomposite conjugated polyaniline and poly(*m*-ferrocenylaniline)-supported palladium nanocatalysts in toluene.

Experimental sections

Synthesis of poly(aniline-co-m-ferrocenylaniline)

m-ferrocenylaniline⁴⁰ was achieved by reduction reaction of m-ferrocenylnitrobenzene⁴¹ with Sn/HCl. To a mixture of aniline (0.51 g, 5.5 mmol) and m-ferrocenylaniline (5, 10, 15, and 20 mol% of aniline) was added 1 M H₂SO₄ (7 cm³). A solution of ammonium peroxydisulfate (1.0 g, 4.4 mmol) in de-ionized water (2 cm³) was added to the suspension. The copolymerization was left stirring under ambient conditions for 24 hours. The precipitate was filtered under vacuum and washed with de-ionized water. The resulting copolymer was dried by incubating at 80 °C for 24 hours.

Synthesis of ferricinium-doped polyaniline

To a suspension of aniline (0.51 g, 5.5 mmol) in 1 M H₂SO₄ (7 cm³) was slowly added 2 cm³ aqueous solution of ammonium peroxydisulfate (1.0 g, 4.4 mmol in de-ionized water). Then, the ferricinium species prepared by dissolving ferrocene (0.51 g, 2.7 mmol) in *conc*. H₂SO₄ (2 cm³) was added to the mixture and the reaction was allowed to proceed upon stirring under ambient conditions. After 24 hours, a fine dark blue-green powder was filtered under vacuum and washed with de-ionized water. The resulting ferricinium-doped polyaniline was dried by incubating at 80 °C for 24 hours.

Synthesis of ferricinium-doped poly(aniline-co-m-ferrocenylaniline)

The experimental procedure was similar to that for polyaniline. A mixture of monomers between aniline (0.51 g, 5.5 mmol) and m-ferrocenylaniline (5, 10, 15, and 20 mol%) was added with 1 M H_2SO_4 (7 cm³). Then, 1 g of ammonium peroxydisulfate in 2

cm³ of de-ionized water was added dropwise into the mixture solution. During the formation of copolymer, the ferricinium ion prepared by mixing ferrocene (0.51 g, 2.74 mmol) in 2 cm³ of *conc*. H₂SO₄ was then added. The copolymerization was allowed to proceed for 24 hours. Then, a fine dark orange precipitate powder was obtained, separated by filtration, and washed several times with water. The resulting copolymer was dried by incubating at 80 °C for 24 hours.

Preparation of palladium nanoparticles (PdNPs)

PdNPs for Suzuki-Miyaura cross-coupling reactions were synthesized by combining palladium(II) acetate (2.2 mg, 0.01 mmol) with polyaniline or poly(aniline-co-m-ferrocenylaniline) (0.1 mmol with respected to their monomer) in 5 cm³ of toluene. The mixture was kept under stirring at ambient temperature for 24 hours.

Suzuki-Miyaura cross-coupling reactions

Arylbromide (0.5 mmol), and arylboronic acid (0.5 mmol) were mixed into 10 cm³ of toluene. A solid of potassium hydroxide (112 mg, 2 mmol) and the PdNPs were added into the reaction flask. The reaction was refluxed for 20 hours. After that, the PdNPs were removed by filtration, and then the filtrant was concentrated under vacuum. All cross-coupling products were characterized by ¹H NMR analysis.

General Characterization

UV-Visible absorption spectra of the sample solution were monitored over the wavelength of 300–800 nm using a HP-8453 Hewlett Packard UV-Visible scanning spectrophotometer with the path length of the quartz cell at 10 mm and dimethyl sulfoxide (DMSO) was used as a reference. A required amount of poly(aniline-*co-m*-ferrocenylaniline)(s) (5 mg) and ferricinium-doped poly(aniline-*co-m*-ferrocenylaniline)(s) (10 mg) was dissolved in DMSO (10 cm³) for the EPR measurements which were performed with a ground sample in a quartz tube. A Bruker (e500) spectrometer was used to operate at

a frequency of 9.86 GHz, and the modulation amplitude used was set at 1.0 G. microwave power for the EPR measurements of the polymers was set at 2.0 mW. The temperature dependence of the EPR signal intensities of the polymers in a solid state was measured at 298 K. In TEM measurements, the sample dispersed in water was dropped on a 300-mesh formvar coated copper grid. The images were acquired by a Tecnai G2 Sphera transmission electron microscope operated at 80 kV. All samples of polymer, ferriciniumdoped polyaniline, poly(aniline-co-m-ferrocenylaniline), ferricinium-doped poly(aniline-copoly(*m*-ferrocenylaniline) ferricinium-doped *m*-ferrocenylaniline), and poly(*m*ferrocenylaniline) were examined by using ¹H NMR spectroscopy (300 MHz and 500 MHz Bruker Avance) with a concentrated solution dissolved in dimethyl sulfoxide- d_6 (DMSO- d_6). The starting materials of Suzuki-Miyaura cross-coupling, m-ferrocenylaniline, mferrocenylnitrobenzene, and all crude products were examined by using chloroform-d (CDCl₃) and methanol- d_4 (CD₃OD). Mass spectra were recorded on a Bruker Data Analysis Esquire-LC mass spectrometer, equipped with an electrospray source using ESI mode and Thermofinnigan Polaris Q 210179 mass spectrometer with direct probe controller 10493 using EI mode. An AUTOLAB-30 electrochemical analyzer was used to carry out the cyclic voltammetric measurements. In all cases, three electrodes were employed, consisting of working electrode and Pt wire serving as a counter electrode and the Ag/AgCl (saturated 3 M KCl) serving as a reference electrode. The electrochemical experiments were carried out at The coercivities (H_c) , the remanent magnetizations (M_r) and the saturation 25 °C. magnetizations (M_s) of the as-prepared samples were performed by using the vibrating sample magnetometer (Lakeshore, Model 4500). The magnetic parameters (H_c , M_r , and M_s) of each sample were determined from the hysteresis loops produced by the vibrating sample magnetometry (VSM). The saturation magnetization was reached at an applied field of 7

kOe. The data of magnetization as a function of the applied field were plotted and also employed for calculations.

Results and Discussion

Poly(aniline-*co-m*-ferrocenylaniline)(s) and poly(*m*-ferrocenylaniline) were readily synthesized in diluted sulfuric acid by using ammonium peroxydisulfate as an oxidant. The structure of poly(aniline-*co-m*-ferrocenylaniline) is proposed as shown in Scheme 1; where Fc is a ferrocenyl substituent on the aromatic ring. Likewise, ferricinium-doped poly(aniline-*co-m*-ferrocenylaniline) was similarly prepared as described above with an external dopant of 50% molar ratio of ferricinium to aniline. The structure of the ferricinium-doped poly(aniline-*co-m*-ferrocenylaniline) is proposed as shown in Scheme 2; where Fc⁺ is a ferricinium species.

UV-Visible spectra of the copolymers were recorded over the range of 300–800 nm as shown in Figure 1. The colorful solutions of poly(aniline-*co-m*-ferrocenylaniline) in DMSO were observed for various molar ratios of *m*-ferrocenylaniline to aniline: green for polyaniline, dark-brown for 5% and 10%, and orange for 15% and 20%. The strong absorption peak is shifted to a lower wavelength at 570 nm for the 5% molar ratio. It can be seen that the blue shift of absorption bands of the copolymers was observed as increasing the molar ratios of *m*-ferrocenylaniline. For 15% and 20% molar ratios of *m*-ferrocenylaniline, the UV-Visible spectra show a strong absorption band at 500 nm which is a characteristic band of orange color of ferrocene moieties.

In order to study the influence of the external dopant of ferricinium ions to the absorption bands of copolymers, the UV-Visible spectra of ferricinium-doped copolymers in DMSO were also monitored. It should be noted that ferricinium ions in *conc*. H₂SO₄ exhibited a blue color. As shown in Figure 2, the solution of ferricinium-doped polymers exhibited two distinct colors: brown-green and orange. The UV-Visible spectra of

ferricinium-doped polyaniline show two absorption bands: the first region of absorption peaks is very broad over the wavelength of 550–700 nm, which is similar to characteristics of polyaniline as described above, ^{42,43} and the second region is located at about 500 nm which is a characteristic of ferrocene obtaining from the reduction from ferricinium ions to ferrocene by polyaniline. This indicated that polyaniline and ferricinium ions can be readily oxidized and reduced, respectively. In contrast, only one absorption band of ferricinium-doped poly(aniline-*co-m*-ferrocenylaniline) was observed at about 500 nm due to the ferrocenyl groups on the polymer backbone and ferricinium-derived ferrocene reduced by polyaniline.

Characteristic EPR spectra of solid polyaniline derivatives are shown in Figure 3. Intensities of the spectra of polyaniline derivatives decreased dramatically as increasing the percentages of *m*-ferrocenylaniline monomers in the structural backbone of poly(aniline-*co-m*-ferrocenylaniline). Compared to polyaniline, the EPR signal of poly(aniline-*co-m*-ferrocenylaniline)(s) became broader and non-symmetrical which strongly depended on the molar ratios of *m*-ferrocenylaniline to aniline. The *g*-values of copolymers were 2.0032, 2.0035, 2.0038, and 2.0039 corresponding to 5%, 10%, 15%, and 20% molar ratio, respectively compared with the *g*-value of polyaniline at 2.0031. Based on the *g*-value obtained from the EPR measurements, it can be described that the addition of *m*-ferrocenylaniline had a minimal influence on the paramagnetic properties of poly(aniline-*co-m*-ferrocenylaniline). The decreasing intensities of EPR spectra of the copolymers may be due to the disorder and the disruption in the conjugation of polymer structures that may cause by the ferrocene moieties on the main chain of the copolymers.

EPR spectra of ferricinium-doped poly(aniline-*co-m*-ferrocenylaniline) were recorded under the same conditions as those measurements of the undoped copolymers. The effect of the ferricinium ion as an external dopant on the EPR intensities of the synthesized-copolymers is shown in Figure 4. The *g*-values of all ferricinium-doped copolymers (2.0034)

were close to the *g*-value of a free electron (2.0036) indicating that the spins over ring and nitrogen repeating units were free electron type and also more delocalized than that of the parent copolymers. However, the *g*-values showed a remarkably small change in ferricinium-doped copolymers revealing that spin orbitals of heteroatoms which contributed to the dynamic defects of ferricinium-doped polymer chains had an almost negligible effect.^{44,45}

The 1 H NMR spectra of polyaniline and its derivatives can be observed in DMSO- d_6 as shown in Figure 5. A triplet peak with the equal intensities at approximately δ 7.3–6.9 ppm was assigned as NH protons of polyaniline which were coupled to 14 N (I = 1). 46 Polyaniline is a good conducting polymer which is easily oxidized and reduced reversibly. 9 Therefore, the paramagnetic ferricinium ions could be reduced to ferrocene by polyaniline as observed by 1 H NMR data. Therefore, two bands in the region of δ 4.2–4.0 ppm were assigned to ferricinium-derived species (Fc $^+$) and ferrocene moiety on the main chain of polymers (Fc), respectively.

In order to compare the conductivity, the undoping and doping processes of the added ferricinium ions were investigated by CV measurements. The electrode was formed by mixing 50 wt% synthetic carbon powder (20 µm diameter), 40 wt% sample and 10 wt% mineral oil as binder before rolling into thin sheet of uniform thickness. The experiments were carried out by repeating potential cycles between –0.1 V and 0.8 V. The CVs at the scan rate of 5 mV·s⁻¹ of the polyaniline and poly(aniline-*co-m*-ferrocenylaniline)(s) with different molar ratios of *m*-ferrocenylaniline to aniline is shown in Figure 6. The peak current was decreased dramatically for 10% molar ratio of *m*-ferrocenylaniline. It can be described that both the steric hindrance to the conjugated length of the polymer and the electron withdrawing power of ferrocene moieties from the aromatic rings could lead to the decreasing of the electron delocalization. It is believed that the ferrocene moiety plays a key role for increasing the oxidizing potential of polymers. However, the current was

increased greatly as increasing the percentages of *m*-ferrocenylaniline. The peak potentials were shifted gradually towards the higher current as increasing the molar ratios of *m*-ferrocenylaniline in the copolymers. It was proposed that these potentials of the assynthesized poly(aniline-*co-m*-ferrocenylaniline)(s) were obtained from the redox process of ferrocenyl moieties⁵⁰ as a part of the structure of poly(aniline-*co-m*-ferrocenylaniline)(s). Therefore, ferrocene and its derivatives were attractive for tuning the redox properties which it can be oxidized and reduced reversibly.

The CV measurements of ferricinium-doped poly(aniline-co-m-ferrocenylaniline) exhibited the redox behavior similarly to the undoped condition as shown in Figure 7. It is clear that the peak current of ferricinium-doped poly(aniline-co-m-ferrocenylaniline) was much lower compared to the ferricinium-doped polyaniline. Moreover, the currents were increased greatly as increasing the percentages of m-ferrocenylaniline in the copolymer. All CV voltammograms display chemically reversible ferrocene/ferricinium redox waves. This was suggested that the ferrocene moieties of copolymers in all samples showed the similar redox potentials due to the lack of direct interactions between the metal centers. Compared to the undoped condition, the higher currents of the doped conditions were observed.

The electron localization effects of the magnetic states in the polyaniline copolymers have been investigated by several studies due to their interesting magnetic behaviors.⁵² Based on the hysteresis loops, the as-prepared poly(aniline-*co-m*-ferrocenylaniline) were soft magnetic materials because the magnetization values obtained from the final products were very low in the range from –0.06 to 0.02 emu/g as shown in Figure 8. As increasing the molar ratio of *m*-ferrocenylaniline in the copolymers, the magnetic behavior from the hysteresis loops tended to increase the electron localization of the as-prepared poly(aniline-*co-m*-ferrocenylaniline)(s).

The general features of the catalytic cycles for Suzuki-Miyaura cross-coupling reactions are currently well understood and involved in the oxidative addition-transmetallation-reductive elimination sequence. ^{15,16} In this study, the Suzuki-Miyaura cross-coupling reactions of aryl bromides and arylboronic acids were catalyzed by heterogeneous palladium nanocatalysts based on the dispersion in the poly(*m*-ferrocenylaniline) as shown in Figure 9. Therefore, ferrocene moieties on the main chain of polymers were expected to accelerate the rate of electron transfer to achieve a higher conversion and selectivity.

The Suzuki-Miyaura cross-coupling reactions of 4-bromotoluene with arylboronic acids were catalyzed by poly(*m*-ferrocenylaniline)-stabilized palladium nanocatalysts under a basic condition at a reflux condition (Scheme 3). The cross-couplings catalyzed by palladium nanocatalysts stabilized by polyaniline were used as a reference. The catalytic studies of Suzuki-Miyaura cross-coupling reactions were summarized in Table 1. The results demonstrated the cross-coupling of 4-bromotoluene and arylboronic acids with PdNPs/polyaniline and PdNPs/poly(*m*-ferrocenylaniline) as a catalyst. It can be expected that the rate of reactions in the entry 2 may be lower than entry 1 due to the electronic and steric effects of the methyl group on the biphenyl ring. Due to this effect, the yields of the polyaniline experiments were expected to be increased from entry 2 to entry 4 which their arylboronic substrates were o-, m-, and p-substituted benzene rings, respectively. Entries 1-3, the poly(m-ferrocenylaniline) experiments gave the excellent conversion and yield percentages higher than the polyaniline experiments while the comparable yields were obtained in both stabilizing ligands for entry 4. Therefore, the ferrocene moieties on the main chain of poly(*m*-ferrocenylaniline) accelerated the rate of reaction by presumably increasing the rate of electron transfer directly to the catalytic sites. Due to the electron withdrawing power of the substituent in Entry 5, the yields were low for both stabilizing ligands. For the entry 6, it was surprising that ferrocene was obtained as a product instead of 4ferrocenyltoluene. This can be proposed that the ferrocene group is liberated from ferrocenylboronic acid in the 2^{nd} transmetallation step⁵³ because no ferrocenylboronic acid was observed in ^{1}H NMR spectrum after the reaction was completed.

Conclusions

A series of novel polyaniline derivatives and copolymers were successfully prepared by a simple oxidative polymerization. The molar ratios of aniline and *m*-ferrocenylaniline have a direct effect on optical, magnetic, and electrical properties of the copolymers. The Suzuki-Miyaura cross-coupling reactions of arylbromide with arylboronic acids in toluene were successfully examined by polyaniline-stabilized PdNPs and poly(*m*-ferrocenylaniline)-stabilized PdNPs as catalysts. For comparison, PdNPs catalysts containing ferrocene moieties were more effective than polyaniline-stabilized PdNPs in the Suzuki-Miyaura cross-coupling.

Acknowledgements

The financial supports by the Research, Development and Engineering (RD&E) fund through the National Nanotechnology Center (NANOTEC), the National Science and Technology Development Agency (NSTDA) (Project No. NN-B-22-FN3-15-52-16), the Thailand Research Fund-the Office of the Higher Education (RMU5380043), Center for Innovation in Chemistry (PERCH-CIC), and the Office of the Higher Education Commission and Mahidol University under the National Research University Initiative are acknowledged.

Note and references

- (1) Tsunoyama, H.; Sakurai, H.; Negishi, Y.; Tsukuda, T. J. Am. Chem. Soc. **2005**, 127, 9374.
- (2) Tsunoyama, H.; Sakurai, H.; Ichikuni, N.; Negishi, Y.; Tsukuda, T. *Langmuir* **2004**, 20, 11293.

- (3) Magdesieva, T. V.; Nikitin, O. M.; Levitsky, O. A.; Zinovyeva, V. A.; Bezverkhyy, I.; Zolotukhina, E. V.; Vorotyntsev, M. A. *J. Mol. Catal. A: Chem.* **2012**, *353*, 50.
- (4) Kantam, M. L.; Roy, M.; Roy, S.; Sreedhar, B.; Madhavendra, S. S.; Choudary, B.M.; De, R. L. *Tetrahedron* **2007**, *63*, 8002.
- (5) Cirtiu, C. M.; Dunlop-Briere, A. F.; Moores, A. *Green Chem.* **2011**, *13*, 288.
- (6) Adeli, M.; Mehdipour, E.; Bavadi, M. J. Appl. Polym. Sci. 2010, 116, 2188.
- (7) Somorjai, G. A.; Park, J. Y. Angew. Chem. Int. Ed. 2008, 47, 9212.
- (8) Chaicharoenwimolkul, L.; Munmai, A.; Chairam, S.; Tewasekson, U.; Sapudom, S.; Lakliang, Y.; Somsook, E. *Tetrahedron Lett.* **2008**, *49*, 7299.
- (9) Handbook of conducting polymer: conjugated polymers, theory, synthesis, properties, and characterization; Skotheim, T. A.; Reynolds, J., Eds.; CRC press: New York, 2007.
- (10) Chen, Z.; Della Pina, C.; Falletta, E.; Lo Faro, M.; Pastaa, M.; Rossi, M.; Santo, N. *J. Catal.* **2008**, 259, 1.
- (11) Cetin, A.; Ortiz-Colon, S.; Espe, M. P.; Ziegler, C. J. Dalton Trans. 2008, 64.
- (12) Han, C. C.; Lu, C. H.; Hong, S. P.; Yang, K. F. *Macromolecules* **2003**, *36*, 7908.
- (13) Amaya, T.; Saio, D.; Koga, S.; Hirao, T. *Macromolecules* **2010**, *43*, 1175.
- (14) Kane-Maguire, L. A. P.; Wallace, G. G. Chem. Soc. Rev. 2010, 39, 2545.
- (15) Miyaura, N.; Suzuki, A. Chem. Rev. 1995, 95, 2457.
- (16) *Metal-catalyzed cross-coupling reactions*; Diederich, F.; Stang, P. J., Eds.; Wiley-VCH: New York, 1998.
- (17) Marziale, A. N.; Faul, S. H.; Reiner, T.; Schneider, S.; Eppinger, J. *Green Chem.* **2010**, *12*, 35.
- (18) Dhara, K.; Sarkar, K.; Srimani, D.; Saha, S. K.; Chattopadhyay, P.; Bhaumik, A. *Dalton Trans.* **2010**, *39*, 6395.
- (19) Nobre, S. M.; Monteiro, A. L. J. Mol. Catal. A: Chem. 2009, 313, 65.

- (20) Tamami, B.; Ghasemi, S. J. Mol. Catal. A: Chem. 2010, 322, 98.
- (21) Gallon, B. J.; Kojima, R. W.; Kaner, R. B.; Diaconescu, P. L. *Angew. Chem. Int. Ed.* **2007**, *46*, 7251.
- (22) Houdayer, A.; Schneider, R.; Billaud, D.; Ghanbaja, J.; Lambert, J. *Appl. Organomet. Chem.* **2005**, *19*, 1239.
- (23) Budroni, G.; Corma, A.; Garia, H.; Primo, A. J. Catal. 2007, 251, 345.
- (24) Kwong, F. Y.; Chan, K. S.; Yeung, C. H.; Chan, A. S. C. *Chem. Commun.* **2004**, 2336.
- (25) Stepnicka, P.; Lamac, M.; Cisarova, I. *Polyhedron* **2004**, *23*, 921.
- (26) Cousaert, N.; Toto, P.; Willand, N.; Deprez, B. Tetrahedron Lett. 2005, 46, 6529.
- (27) Sliger, M. D.; Broker, G. A.; Griffin, S. T.; Rogers, R. D.; Shaughnessy, K. H. *J. Organomet. Chem.* **2005**, *690*, 1478.
- (28) Shi, J. C.; Yang, P. Y.; Tong, Q. S.; Wu, Y.; Peng, Y. J. Mol. Catal. A: Chem. 2006, 259, 7.
- (29) Wang, H. X.; Wu, H. F.; Yang, X. L.; Ma, N.; Wan, L. *Polyhedron* **2007**, *26*, 3857.
- (30) Punji, B.; Mague, J. T.; Balakrishna, M. S. *Inorg. Chem.* **2007**, *46*, 10268.
- (31) Kuhnert, J.; Lamac, M.; Demel, J.; Nicolai, A.; Lang, H.; Stepnicka, P. *J. Mol. Catal. A: Chem.* **2008**, 285, 41.
- (32) Garabatos-Perera, J. R.; Butenschon, H. J. Organomet. Chem. 2008, 693, 357.
- (33) Yu, S. B.; Hu, X. P.; Deng, J.; Huang, J. D.; Wang, D. Y.; Duan, Z. C.; Zheng, Z. *Tetrahedron Lett.* **2008**, *49*, 1253.
- (34) Stepnicka, P.; Krupa, M.; Lamac, M.; Cisarova, I. *J. Organomet. Chem.* **2009**, 694, 2987.
- (35) Tauchman, J.; Cisarova, I.; Stepnicka, P. Organometallics 2009, 28, 3288.
- (36) Schulz, J.; Cisarova, I.; Stepnicka, P. J. Organomet. Chem. 2009, 694, 2519.

- (37) Mu, B.; Li, T. S.; Li, C. H.; Liu, P. P.; Shang, W.; Wu, Y. J. *Tetrahedron* **2009**, *65*, 2599.
- (38) Stepnicka, P.; Schulz, J.; Klemann, T.; Siemeling, U.; Cisarova, I. *Organometallics* **2010**, *29*, 3187.
- (39) Ren, G. R.; Cui, X. L.; Wu, Y. J. Eur. J. Org. Chem. 2010, 2372.
- (40) Asaro, M. F.; Nakayama, I.; Wilson, R. B. J. Org. Chem. 1992, 57, 778.
- (41) Savage, D.; Alley, S. R.; Gallagher, J. F.; Goel, A.; Kelly, P. N.; Kenny, P. T. M. *Inorg. Chem. Commun.* **2006**, *9*, 152.
- (42) Ali Shah, A. U. H.; Holze, R. Synth. Met. 2006, 156, 566.
- (43) Amaya, T.; Saio, D.; Hirao, T. *Tetrahedron Lett.* **2007**, 48, 2729.
- (44) Scott, J. C.; Pfluger, P.; Krounbi, M. T.; Street, G. B. Phys. Rev. B 1983, 28, 2140.
- (45) Jeevananda, T.; Siddaramaiah; Seetharamu, S.; Saravanan, S.; D'Souza, L. *Synth. Met.* **2004**, *140*, 247.
- (46) Zhang, J.; Shan, D.; Mu, S. L. *Polymer* **2007**, *48*, 1269.
- (47) Petersen, R.; Foucher, D. A.; Tang, A.-Z.; Lough, A.; Raju, N. P.; Greedan, J. E.; Manners, I. *Chem. Mater.* **1995**, *7*, 2045.
- (48) Lee, H. Y.; Goodenough, J. B. J Solid State Chem. 1999, 144, 220.
- (49) Xu, Y.; Dai, L.; Chen, J.; Gal, J.-Y.; Wu, H. Eur. Polym. J. **2007**, 43, 2072.
- (50) Shi, J.; Tong, B.; Zhao, W.; Shen, J.; Zhi, J.; Dong, Y.; Haussler, M.; Lam, J. W. Y.; Tang, B. Z. *Macromolecules* **2007**, *40*, 5612.
- (51) EL Sayed, A. M.; Yamasaki, S.; Yamauchi, A. J. Appl. Polym. Sci. 2008, 107, 1678.
- (52) Kahol, P. K.; Pendse, V.; Pinto, N. J.; Traore, M.; Stevenson, W. T. K.; McCormick,B. J.; Gundersen, J. N. *Phys. Rev. B* 1994, *50*, 2809.
- (53) Braga, A. A. C.; Ujaque, G.; Maseras, F. *Organometallics* **2006**, *25*, 3647.



Effect of Ferrocene Substituents and Ferricinium Additive on the Properties of Polyaniline Derivatives and Catalytic Activities of Palladium-Doped Poly(m-ferrocenylaniline)-Catalyzed Suzuki-Miyaura Cross-Coupling Reactions

Laksamee Chaicharoenwimolkul,^{1,2} Sanoe Chairam,³ Montree Namkajorn,¹ Achjana Khamthip,¹ Choavarit Kamonsatikul,¹ Udomchai Tewasekson,¹ Sudarat Jindabot,¹ Weeraphat Pon-On,¹ Ekasith Somsook¹

¹NANOCAST Laboratory, Center for Catalysis, Department of Chemistry and Center for Innovation in Chemistry, Faculty of Science, Mahidol University, 272 Rama VI Rd., Thung Phaya Thai, Ratchathewi, Bangkok 10400, Thailand

²School of Chemistry, Faculty of Science and Technology, Suratthani Rajabhat University, 272 Moo 9, Surat-Nasan Rd., Khuntale, Muang, Surat Thani 84100, Thailand

³Department of Chemistry and Center for Innovation in Chemistry, Faculty of Science, Ubon Ratchathani University, Warinchamrap, Ubon Ratchathani 34190, Thailand

Correspondence to: E. Somsook (E-mail: ekasith.som@mahidol.ac.th)

ABSTRACT: Poly(aniline-co-m-ferrocenylaniline) and ferricinium-doped poly(aniline-co-m-ferrocenylaniline) were synthesized by a conventional chemical oxidative polymerization, then characterized by spectroscopic techniques and quantitative analyzes. Increasing of the percentages of m-ferrocenylaniline in the copolymers resulted to a blue shift of UV–Vis absorption spectra. Broader EPR spectra indicated the loss of conjugation and crystallinity of copolymers. ¹H NMR spectra confirmed the presence of ferrocene moieties and ferricinium in the polymers. The CV measurements showed that the electron withdrawing power of ferrocene moieties could lead to the decreasing of electron delocalization on the polymer main chain. The VSM results showed that as-prepared copolymers were soft magnetic materials with very low magnetization. Pd-doped poly(m-ferrocenylaniline) as catalysts were utilized in the Suzuki–Miyaura cross-coupling reactions to improve the catalytic activities. © 2013 Wiley Periodicals, Inc. J. Appl. Polym. Sci. 130: 1489–1497, 2013

KEYWORDS: nanoparticles; nanowires and nanocrystals; catalysts; non-polymeric materials and composites

Received 19 November 2012; accepted 10 March 2013; Published online 29 April 2013

DOI: 10.1002/app.39279

INTRODUCTION

It is of special interest to investigate hybrid nanocomposites based on organic polymers which can be fabricated with various inorganic nanoparticles to create nanocatalysts with improvements in their properties for catalysis. ^{1–6} In addition to the size and shape of nanocatalysts, it is apparent that some molecular factors such as the surface composition, charge transfer, and oxidation state of the stabilizing ligand layers can be used to control the catalytic activity and selectivity of nanocatalysts⁷ which can be chemically tuned with the redox property of appropriate ligands or polymers. ⁸ Polyaniline ⁹ is currently an excellent example of the most widely studied conducting polymers which can be synthesized by the oxidative polymerization of aniline in an aqueous acid solution with ease, either by using an electrochemical method or a chemical oxidant polymerization. ^{10,11} In

order to modify the properties of polymers, substituted polyanilines can be made by adding various functional groups to the backbone of the polymers or incorporating external dopants binding to the polymer backbone.^{12–14}

The Suzuki–Miyaura cross-coupling reaction of aryl halides with arylboronic acids is a fundamental transformation in modern organic synthesis and offers a powerful method for the aryl–aryl formation. ^{15,16} Palladium complexes and nanoparticles are one of the most useful catalysts for carbon–carbon cross-coupling reactions. ^{3–5,17–20} Recently, conjugated conductive polyaniline used as a supporter for palladium nanoparticles (PdNPs) has been reported as excellent catalysts in the cross-coupling reactions. ^{4,21–23} A number of studies investigated ligands containing ferrocene covalently bonded for the metal-assisted cross-coupling reactions of aryl halides with arylboronic

© 2013 Wiley Periodicals, Inc.



acids.^{24–39} As part of our efforts to synthesize a novel conjugated polymer, herein polyanilines based on the redox-active ferrocene moiety extended on the polymer backbone were synthesized, and their properties were investigated to improve the catalytic activities. The aims of this study were therefore to prepare and characterize poly(aniline-co-m-ferrocenylaniline)(s) and ferricinium-doped poly(aniline-co-m-ferrocenylaniline)(s), and investigate the Suzuki–Miyaura cross-coupling activities catalyzed by the nanocomposite conjugated polyaniline and poly(m-ferrocenylaniline)-supported palladium nanocatalysts in toluene.

EXPERIMENTAL

Synthesis of Poly(aniline-co-m-ferrocenylaniline)

m-Ferrocenylaniline 40 was achieved by reduction reaction of m-ferrocenylnitrobenzene 41 with Sn/HCl. To a mixture of aniline (0.51 g, 5.5 mmol) and m-ferrocenylaniline (5, 10, 15, and 20 mol % of aniline) was added 1 M H₂SO₄ (7 cm³). A solution of ammonium peroxydisulfate (1.0 g, 4.4 mmol) in de-ionized water (2 cm³) was added to the suspension. The copolymerization was left stirring under ambient conditions for 24 h. The precipitate was filtered under vacuum and washed with de-ionized water. The resulting copolymer was dried by incubating at 80° C for 24 h.

Synthesis of Ferricinium-Doped Polyaniline

To a suspension of aniline (0.51 g, 5.5 mmol) in 1*M* H₂SO₄ (7 cm³) was slowly added 2 cm³ aqueous solution of ammonium peroxydisulfate (1.0 g, 4.4 mmol in de-ionized water). Then, the ferricinium species prepared by dissolving ferrocene (0.51 g, 2.7 mmol) in *conc.* H₂SO₄ (2 cm³) was added to the mixture and the reaction was allowed to proceed upon stirring under ambient conditions. After 24 h, a fine dark blue-green powder was filtered under vacuum and washed with de-ionized water. The resulting ferricinium-doped polyaniline was dried by incubating at 80°C for 24 h.

Synthesis of FerriciniumDoped Poly(aniline-co-m-ferrocenylaniline)

The experimental procedure was similar to that for polyaniline. A mixture of monomers between aniline (0.51 g, 5.5 mmol) and *m*-ferrocenylaniline (5, 10, 15, and 20 mol %) was added with 1*M* H₂SO₄ (7 cm³). Then, 1 g of ammonium peroxydisulfate in 2 cm³ of de-ionized water was added dropwise into the mixture solution. During the formation of copolymer, the ferricinium ion prepared by mixing ferrocene (0.51 g, 2.74 mmol) in 2 cm³ of *conc*. H₂SO₄ was then added. The copolymerization was allowed to proceed for 24 h. Then, a fine dark orange precipitate powder was obtained, separated by filtration, and washed several times with water. The resulting copolymer was dried by incubating at 80°C for 24 h.

Preparation of Palladium Nanoparticles (PdNPs)

PdNPs for Suzuki–Miyaura cross-coupling reactions were synthesized by combining palladium(II) acetate (2.2 mg, 0.01 mmol) with polyaniline or poly(aniline-*co-m*-ferrocenylaniline) (0.1 mmol with respected to their monomer) in 5 cm³ of

toluene. The mixture was kept under stirring at ambient temperature for 24 h.

Suzuki-Miyaura Cross-Coupling Reactions

Arylbromide (0.5 mmol) and arylboronic acid (0.5 mmol) were mixed into 10 cm³ of toluene. A solid of potassium hydroxide (112 mg, 2 mmol) and the PdNPs were added into the reaction flask. The reaction was refluxed for 20 h. After that, the PdNPs were removed by filtration, and then the filtrant was concentrated under vacuum. All cross-coupling products were characterized by ¹H NMR analysis.

General Characterization

UV-Visible absorption spectra of the sample solution were monitored over the wavelength of 300-800 nm using a HP-8453 Hewlett Packard UV-Visible scanning spectrophotometer with the path length of the quartz cell at 10 mm and dimethyl sulfoxide (DMSO) was used as a reference. A required amount of poly(aniline-co-m-ferrocenylaniline)(s) (5 mg) and ferriciniumdoped poly(aniline-co-m-ferrocenylaniline)(s) (10 mg) was dissolved in DMSO (10 cm³) for the EPR measurements which were performed with a ground sample in a quartz tube. A Bruker (e500) spectrometer was used to operate at a frequency of 9.86 GHz, and the modulation amplitude used was set at 1.0 G. The microwave power for the EPR measurements of the polymers was set at 2.0 mW. The temperature dependence of the EPR signal intensities of the polymers in a solid state was measured at 298 K. In TEM measurements, the sample dispersed in water was dropped on a 300-mesh formvar coated copper grid. The images were acquired by a Tecnai G2 Sphera transmission electron microscope operated at 80 kV. All samples of polymer, ferricinium-doped polyaniline, poly(aniline-co-mferrocenylaniline), ferricinium-doped poly(aniline-co-m-ferrocenylaniline), poly(m-ferrocenylaniline), and ferricinium-doped poly(*m*-ferrocenylaniline) were examined by using ¹H NMR spectroscopy (300 and 500 MHz Bruker Avance) with a concentrated solution dissolved in dimethyl sulfoxide- d_6 (DMSO- d_6). The starting materials of Suzuki-Miyaura cross-coupling, m-ferrocenylaniline, m-ferrocenylnitrobenzene, and all crude products were examined by using chloroform-d (CDCl₃) and methanol d_4 (CD₃OD). Mass spectra were recorded on a Bruker Data Analysis Esquire-LC mass spectrometer, equipped with an electrospray source using ESI mode and Thermofinnigan Polaris Q 210179 mass spectrometer with direct probe controller 10493 using EI mode. An AUTOLAB-30 electrochemical analyzer was used to carry out the cyclic voltammetric measurements. In all cases, three electrodes were employed, consisting of working electrode and Pt wire serving as a counter electrode and the Ag/ AgCl (saturated 3M KCl) serving as a reference electrode. The electrochemical experiments were carried out at 25°C. The coercivities (H_c) , the remanent magnetizations (M_r) , and the saturation magnetizations (M_s) of the as-prepared samples were performed by using the vibrating sample magnetometer (Lakeshore, Model 4500). The magnetic parameters $(H_0, M_p, \text{ and } M_s)$ of each sample were determined from the hysteresis loops produced by the vibrating sample magnetometry (VSM). The saturation magnetization was reached at an applied field of 7 kOe. The data of magnetization as a function of the applied field were plotted and also employed for calculations.



Applied Polymer Article

Scheme 1. The preparation of poly(aniline-co-m-ferrocenylaniline).

RESULTS AND DISCUSSION

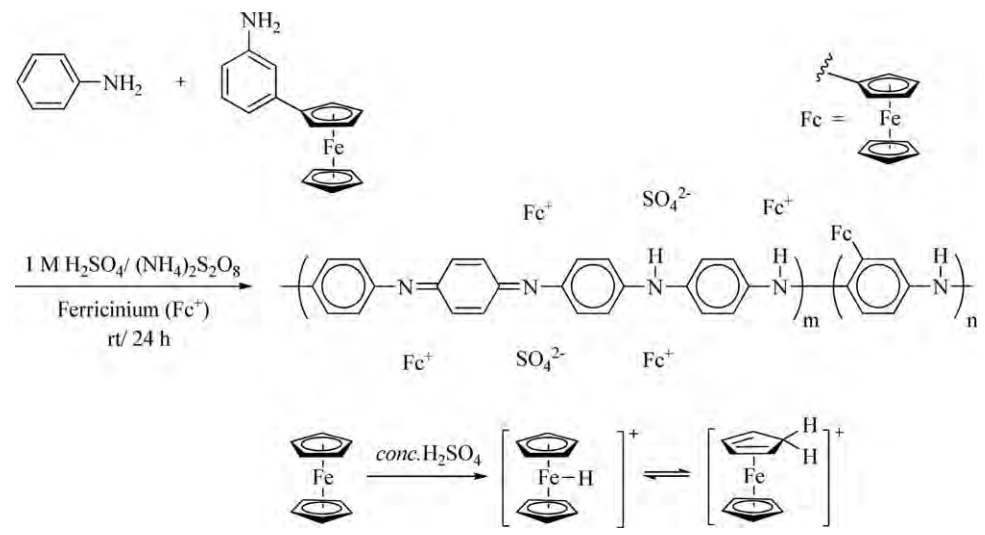
Poly(aniline-*co-m*-ferrocenylaniline)(s) and poly(*m*-ferrocenylaniline) were readily synthesized in diluted sulfuric acid by using ammonium peroxydisulfate as an oxidant. The structure of poly(aniline-*co-m*-ferrocenylaniline) is proposed as shown in Scheme 1; where Fc is a ferrocenyl substituent on the aromatic ring. Likewise, ferricinium-doped poly(aniline-*co-m*-ferrocenylaniline) was similarly prepared as described above with an external dopant of 50% molar ratio of ferricinium to aniline. The structure of the ferricinium-doped poly(aniline-*co-m*-ferrocenylaniline) is proposed as shown in Scheme 2; where Fc⁺ is a ferricinium species.

UV–Visible spectra of the copolymers were recorded over the range of 300–800 nm as shown in Figure 1. The colorful solutions of poly(aniline-co-m-ferrocenylaniline) in DMSO were observed for various molar ratios of m-ferrocenylaniline to aniline: green for polyaniline, dark-brown for 5 and 10%, and orange for 15 and 20%. The strong absorption peak is shifted to a lower wavelength at 570 nm for the 5% molar ratio. It can be seen that the blue shift of absorption bands of the copolymers was observed as increasing the molar ratios of m-ferrocenylaniline. For 15 and 20% molar ratios of m-ferrocenylaniline, the UV–Visible spectra show a strong absorption band at 500 nm

which is a characteristic band of orange color of ferrocene moieties.

In order to study the influence of the external dopant of ferricinium ions to the absorption bands of copolymers, the UV-Visible spectra of ferricinium-doped copolymers in DMSO were also monitored. It should be noted that ferricinium ions in conc. H₂SO₄ exhibited a blue color. In Figure 2, the solution of ferricinium-doped polymers exhibited two distinct colors: brown-green and orange. The UV-Visible spectra of ferricinium-doped polyaniline show two absorption bands: the first region of absorption peaks is very broad over the wavelength of 550-700 nm, which is similar to characteristics of polyaniline as described above, 42,43 and the second region is located at about 500 nm which is a characteristic of ferrocene obtaining from the reduction from ferricinium ions to ferrocene by polyaniline. This indicated that polyaniline and ferricinium ions can be readily oxidized and reduced, respectively. In contrast, only one absorption band of ferricinium-doped poly(aniline-co-mferrocenylaniline) was observed at about 500 nm due to the ferrocenyl groups on the polymer backbone and ferriciniumderived ferrocene reduced by polyaniline.

Characteristic EPR spectra of solid polyaniline derivatives are shown in Figure 3. Intensities of the spectra of polyaniline



Scheme 2. The preparation of ferricinium-doped poly(aniline-co-m-ferrocenylaniline).

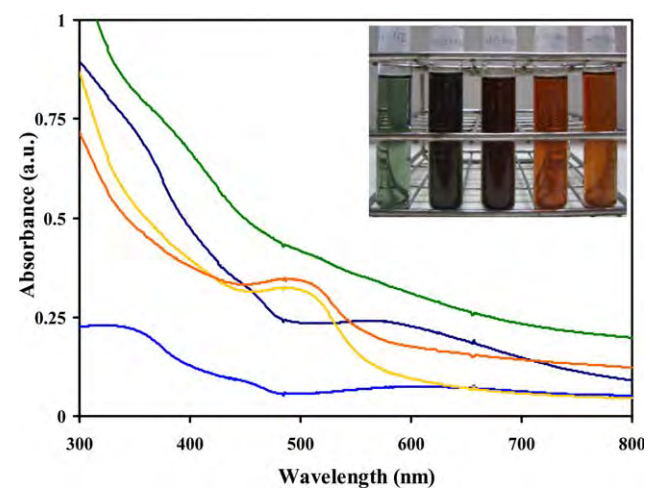


Figure 1. UV-Visible spectra of poly(aniline-co-m-ferrocenylaniline) for (----) 0%, (-----) 5%, (-----) 10%, (-----) 15%, and (------) 20% molar ratios of m-ferrocenylaniline to aniline. Each solution contains a 5 mg of the sample dissolved in DMSO (10 cm³). [Color figure can be viewed in the online issue, which is available at wileyonlinelibrary.com.]

derivatives decreased dramatically as increasing the percentages of m-ferrocenylaniline monomers in the structural backbone of poly(aniline-co-m-ferrocenylaniline). Compared to polyaniline, the EPR signal of poly(aniline-co-m-ferrocenylaniline)(s) became broader and non-symmetrical which strongly depended on the molar ratios of m-ferrocenylaniline to aniline. The g-values of copolymers were 2.0032, 2.0035, 2.0038, and 2.0039 corresponding to 5, 10, 15, and 20% molar ratio, respectively compared with the g-value of polyaniline at 2.0031. Based on the g-value obtained from the EPR measurements, it can be described that the addition of *m*-ferrocenylaniline had a minimal influence on the paramagnetic properties of poly(aniline-co-m-ferrocenylaniline). The decreasing intensities of EPR spectra of the

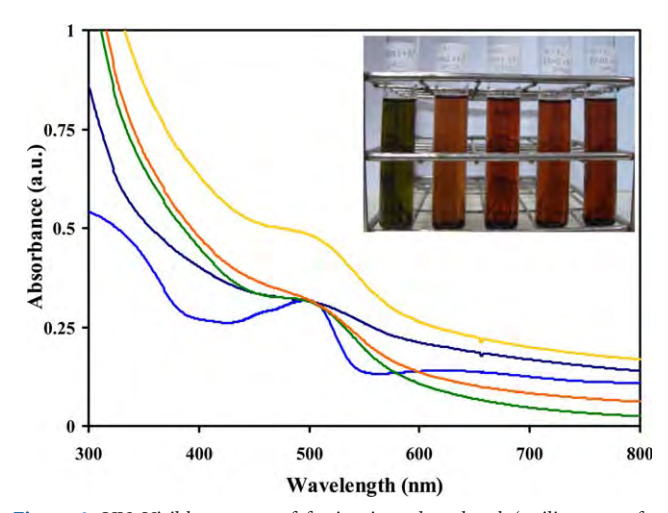


Figure 2. UV-Visible spectra of ferricenium-doped poly(aniline-co-m-ferrocenylaniline) for () 0%, () 5%, () 10%, () 15%, and (-----) 20% molar ratio of m-ferrocenylaniline to aniline. Each solution contains a 10 mg of the sample dissolved in DMSO (10 cm³). [Color figure can be viewed in the online issue, which is available at wileyonlinelibrary.com.]

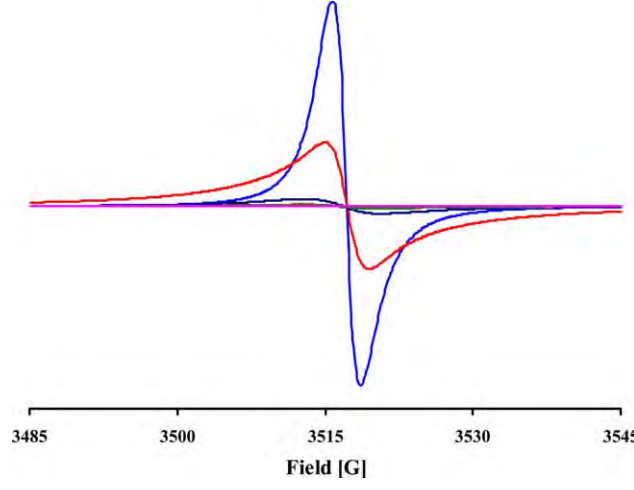


Figure 3. EPR spectra of poly(aniline-co-m-ferrocenylaniline)(s) for () 0%, () 5%, () 10%, () 15%, () 20% molar ratio of *m*-ferrocenylaniline to aniline, and (_____) poly(*m*-ferrocenylaniline). [Color figure can be viewed in the online issue, which is available at wileyonlinelibrary.com.]

copolymers may be due to the disorder and the disruption in the conjugation of polymer structures that may cause by the ferrocene moieties on the main chain of the copolymers.

EPR spectra of ferricinium-doped poly(aniline-co-m-ferrocenylaniline) were recorded under the same conditions as those measurements of the undoped copolymers. The effect of the ferricinium ion as an external dopant on the EPR intensities of the synthesized-copolymers is shown in Figure 4. The g-values of all ferricinium-doped copolymers (2.0034) were close to the g-value of a free electron (2.0036) indicating that the spins over ring and nitrogen repeating units were free electron type and also more delocalized than that of the parent copolymers.

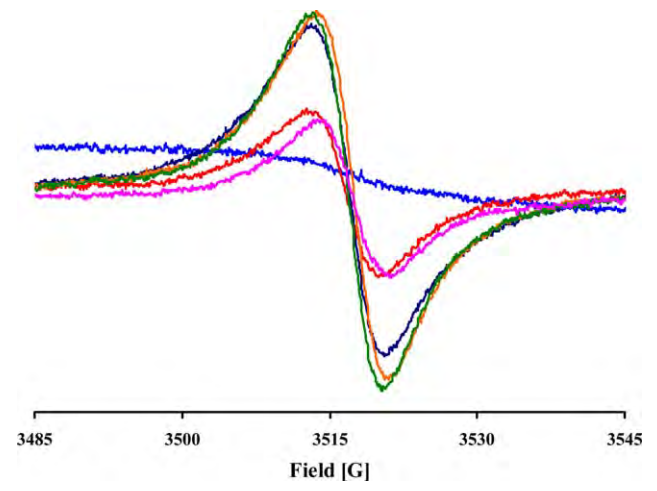


Figure 4. EPR spectra of ferricinium-doped to poly(aniline-co-m-ferrocenylaniline)(s) for (_____) 0%, (_____) 5%, (______) 10%, (______) 15%, (20% molar ratio of *m*-ferrocenylaniline to aniline, and () poly(m-ferrocenylaniline). [Color figure can be viewed in the online issue, which is available at wileyonlinelibrary.com.]

Applied Polymer Article

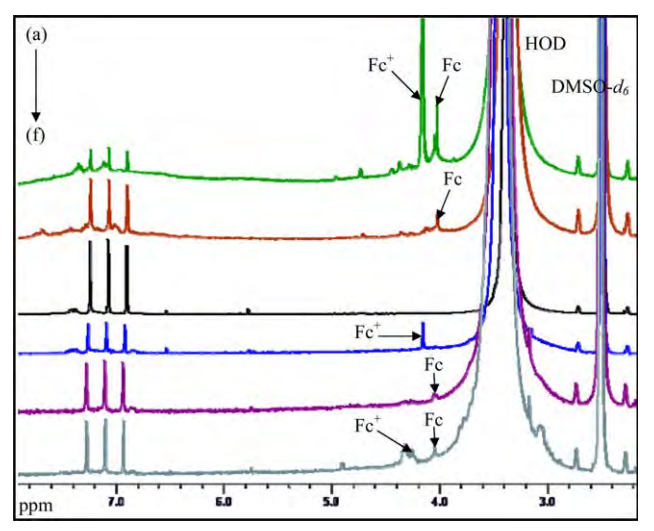


Figure 5. ¹H NMR spectra of (a) ferricinium-doped poly(aniline-co-20%m-ferrocenylaniline), (b) poly(aniline-co-20%m-ferrocenylaniline), (c) polyaniline, (d) ferricinium-doped polyaniline, (e) poly(m-ferrocenylaniline), and (f) ferricinium-doped poly(m-ferrocenylaniline). [Color figure can be viewed in the online issue, which is available at wileyonlinelibrary. com.]

However, the g-values showed a remarkably small change in ferricinium-doped copolymers revealing that spin orbitals of heteroatoms which contributed to the dynamic defects of ferricinium-doped polymer chains had an almost negligible effect. 44,45

The ^1H NMR spectra of polyaniline and its derivatives can be observed in DMSO- d_6 as shown in Figure 5. A triplet peak with the equal intensities at approximately δ 7.3–6.9 ppm was assigned as NH protons of polyaniline which were coupled to ^{14}N (I=1). Polyaniline is a good conducting polymer which is easily oxidized and reduced reversibly. Therefore, the paramagnetic ferricinium ions could be reduced to ferrocene by polyaniline as observed by ^1H NMR data. Therefore, two bands in the region of δ 4.2–4.0 ppm were assigned to ferricinium-derived species (Fc⁺) and ferrocene moiety on the main chain of polymers (Fc), respectively.

In order to compare the conductivity, the undoping and doping processes of the added ferricinium ions were investigated by CV measurements. The electrode was formed by mixing 50 wt% synthetic carbon powder (20 μ m diameter), 40 wt % sample and 10 wt % mineral oil as binder before rolling into thin sheet of uniform thickness. ^{47,48} The experiments were carried out by repeating potential cycles between -0.1 V and 0.8 V. The CVs at the scan rate of 5 mVs⁻¹ of the polyaniline and poly(aniline-co-m-ferrocenylaniline)(s) with different molar ratios of m-ferrocenylaniline to aniline is shown in Figure 6. The peak current was decreased dramatically for 10% molar ratio of m-ferrocenylaniline. It can be described that both the sterichindrance to the conjugated length of the polymer and the electron withdrawing power of ferrocene moieties from the aromatic rings could lead

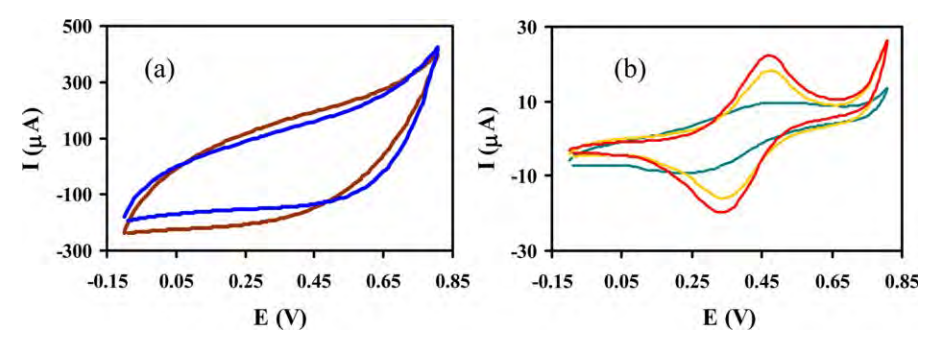


Figure 6. Cyclic voltammograms of poly(aniline-co-m-ferrocenylaniline)(s); (a) for (\longrightarrow) 0%, (\longrightarrow) 5%, (b) for (\longrightarrow) 10%, (\longrightarrow) 15%, and (\longrightarrow) 20% molar ratio of m-ferrocenylaniline to aniline in 0.1M KCl at the scan rate of 5 mVs⁻¹. [Color figure can be viewed in the online issue, which is available at wileyonlinelibrary.com.]

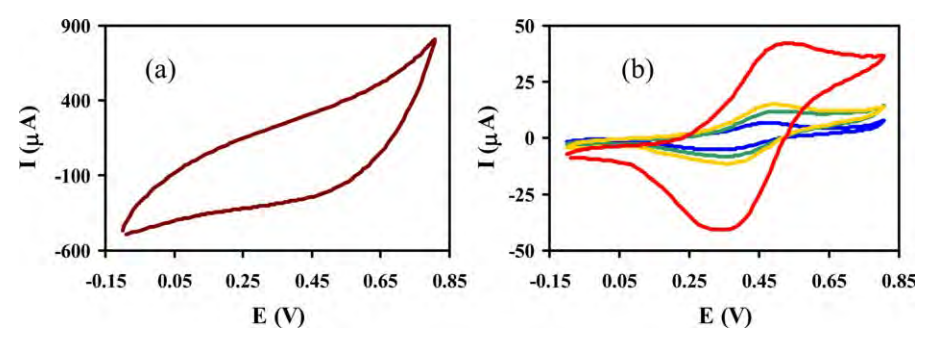


Figure 7. Cyclic voltammograms of ferricinium-doped poly(aniline-*co-m*-ferrocenylaniline) (a) for (——) 0%, (b) for (——) 5%, (——) 10%, (——) 15%, and (——) 20% molar ratio of *m*-ferrocenylaniline in 0.1*M* KCl at the scan rate of 5 mV·s⁻¹. [Color figure can be viewed in the online issue, which is available at wileyonlinelibrary.com.]



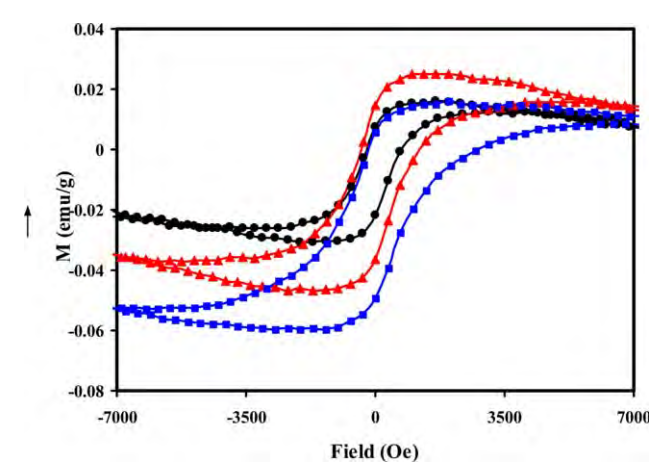


Figure 8. Hysteresis loops at 300 K of poly(aniline-*co-m*-ferrocenylaniline)(s) for (\longrightarrow 5%, (\longrightarrow 10%, and (\longrightarrow 20% of *m*-ferrocenylaniline by molar ratio to aniline. The magnetic parameters of 5, 10, and 20%, respectively: H_c (G) 476.74, 790.40, 1,474.4; M_s (emu/g) 23.265 × 10^{-3} , 35.930 × 10^{-3} , 37.923 × 10^{-3} ; M_r (emu/g) 14.472 × 10^{-3} , 25.238 × 10^{-3} , 27.272 × 10^{-3} . [Color figure can be viewed in the online issue, which is available at wileyonlinelibrary.com.]

to the decreasing of the electron delocalization.⁴⁹ It is believed that the ferrocene moiety plays a key role for increasing the oxidizing potential of polymers. However, the current was increased greatly as increasing the percentages of *m*-ferrocenylaniline. The peak potentials were shifted gradually towards the higher current as increasing the molar ratios of *m*-ferrocenylaniline in the copolymers. It was proposed that these potentials of the as-synthesized poly(aniline-*co-m*-ferrocenylaniline)(s) were obtained from the redox process of ferrocenyl moieties⁵⁰ as a part of the structure of poly(aniline-*co-m*-ferrocenylaniline)(s). Therefore, ferrocene and its derivatives were attractive for tuning the redox properties which it can be oxidized and reduced reversibly.

The CV measurements of ferricinium-doped poly(aniline-co-m-ferrocenylaniline) exhibited the redox behavior similarly to the undoped condition as shown in Figure 7. It is clear that the peak current of ferricinium-doped poly(aniline-co-m-ferrocenylaniline) was much lower compared to the ferricinium-doped polyaniline. Moreover, the currents were increased greatly as increasing the percentages of m-ferrocenylaniline in the copolymer. All CV voltammograms display chemically reversible ferrocene/ferricinium redox waves. This was suggested that the ferrocene moieties of copolymers in all samples showed the similar redox potentials due to the lack of direct interactions between the metal centers. Compared to the undoped condition, the higher currents of the doped conditions were observed.

The electron localization effects of the magnetic states in the polyaniline copolymers have been investigated by several studies due to their interesting magnetic behaviors. Based on the hysteresis loops, the as-prepared poly(aniline-co-m-ferrocenylaniline) were soft magnetic materials because the magnetization values obtained from the final products were very low in the range from -0.06 to 0.02 emu/g as shown in Figure 8. As

increasing the molar ratio of m-ferrocenylaniline in the copolymers, the magnetic behavior from the hysteresis loops tended to increase the electron localization of the as-prepared poly(aniline-co-m-ferrocenylaniline)(s).

The general features of the catalytic cycles for Suzuki–Miyaura cross-coupling reactions are currently well understood and involved in the oxidative addition–transmetallation–reductive elimination sequence. ^{15,16} In this study, the Suzuki–Miyaura cross-coupling reactions of aryl bromides and arylboronic acids were catalyzed by heterogeneous palladium nanocatalysts based on the dispersion in the poly(*m*-ferrocenylaniline) as shown in Figure 9. Therefore, ferrocene moieties on the main chain of polymers were expected to accelerate the rate of electron transfer to achieve a higher conversion and selectivity.

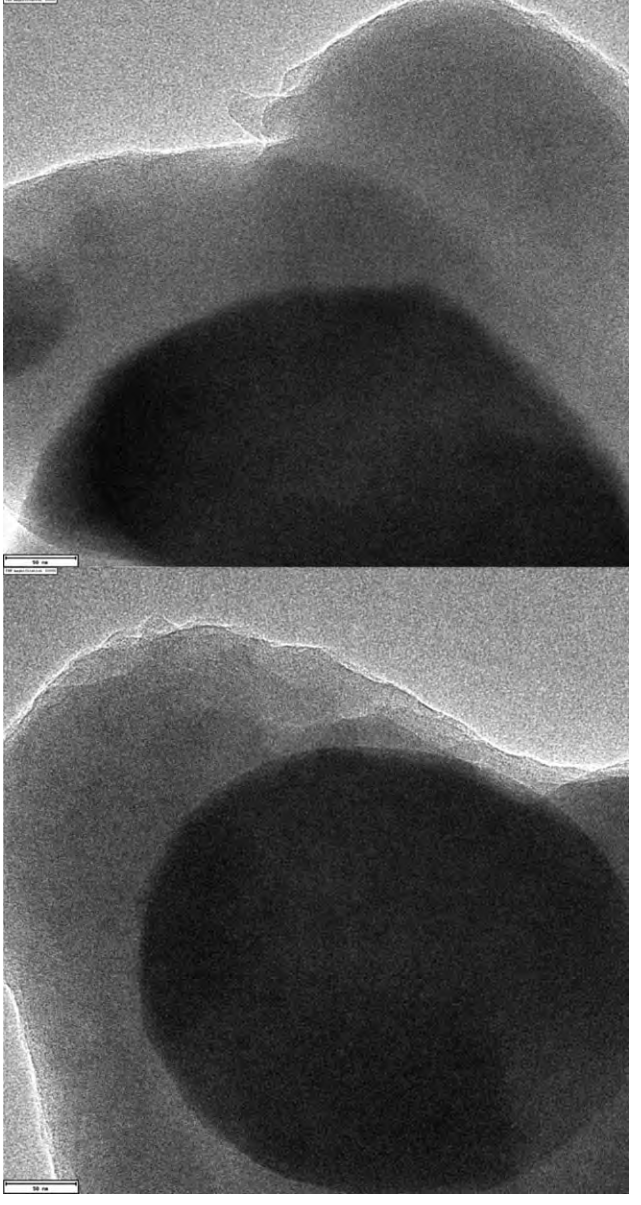


Figure 9. TEM image of Pd-doped poly(*m*-ferrocenylaniline). Bar is 50 nm.

Applied Polymer Article

Scheme 3. Suzuki-Miyaura cross-coupling reactions of 4-bromotoluene with arylboronic acids.

The Suzuki–Miyaura cross-coupling reactions of 4-bromotoluene with arylboronic acids were catalyzed by poly(*m*-ferrocenylaniline)-stabilized palladium nanocatalysts under a basic condition at a reflux condition (Scheme 3). The cross-couplings catalyzed by palladium nanocatalysts stabilized by polyaniline were used as a reference. The catalytic studies of Suzuki–Miyaura cross-coupling reactions were summarized in Table I. The results demonstrated the cross-coupling of 4-bromotoluene and arylboronic acids with PdNPs/polyaniline and PdNPs/poly(*m*-ferrocenylaniline) as a catalyst. It can be expected that the rate of reactions in the entry 2 may be lower than entry 1 due to the electronic and steric effects of the methyl group on the biphenyl ring. Due to this effect, the yields of the polyaniline experiments were expected to be increased from entry 2 to entry 4 which their arylboronic substrates were *o*-, *m*-, and *p*-

substituted benzene rings, respectively. Entries 1–3, the poly(*m*-ferrocenylaniline) experiments gave the excellent conversion and yield percentages higher than the polyaniline experiments while the comparable yields were obtained in both stabilizing ligands for entry 4. Therefore, the ferrocene moieties on the main chain of poly(*m*-ferrocenylaniline) accelerated the rate of reaction by presumably increasing the rate of electron transfer directly to the catalytic sites. Due to the electron withdrawing power of the substituent in entry 5, the yields were low for both stabilizing ligands. For the entry 6, it was surprising that ferrocene was obtained as a product instead of 4-ferrocenyltoluene. This can be proposed that the ferrocene group is liberated from ferrocenylboronic acid in the second transmetallation step⁵³ because no ferrocenylboronic acid was observed in ¹H NMR spectrum after the reaction was completed.

Table I. Suzuki–Miyaura Cross-Coupling of 4-Bromotoluene and Arylboronic Acids with Polyaniline (1) or Poly(*m*-ferrocenylaniline) (2) as Stabilizing Ligand

				%Yield ^a	
Entry	R ₁ -X	R_2 -B(OH) ₂	Product	PdNPs/1	PdNPs/2
1		B(OH) ₂	€ CH ₃	81	>99
2		CH_3 $B(OII)_2$	CH ₃	67	>99
3	Br CH ₃	H ₃ C B(OH) ₂	H ₃ C CH ₃	92	>99
4		H_3C \longrightarrow $B(OH)_2$	H ₃ C ————————————————————————————————————	98	>99
5		O H B(OH) ₂	O CH_3	26	24
6		Fe	Fe	69	92

The reaction conditions were refluxed for 20 h with 4 equiv. KOH in toluene (10 cm³).

^a Estimated from ¹H NMR analysis.



1495

CONCLUSIONS

A series of novel polyaniline derivatives and copolymers were successfully prepared by a simple oxidative polymerization. The molar ratios of aniline and *m*-ferrocenylaniline have a direct effect on optical, magnetic, and electrical properties of the copolymers. The Suzuki–Miyaura cross-coupling reactions of arylbromide with arylboronic acids in toluene were successfully examined by polyaniline-stabilized PdNPs and poly(*m*-ferrocenylaniline)-stabilized PdNPs as catalysts. For comparison, PdNPs catalysts containing ferrocene moieties were more effective than polyaniline-stabilized PdNPs in the Suzuki–Miyaura cross-coupling.

ACKNOWLEDGMENTS

The financial supports by the Research, Development and Engineering (RD&E) fund through the National Nanotechnology Center (NANOTEC), the National Science and Technology Development Agency (NSTDA) (Project No. NN-B-22-FN3–15-52-16), the Thailand Research Fund-the Office of the Higher Education (RMU5380043), Center for Innovation in Chemistry (PERCH-CIC), and the Office of the Higher Education Commission and Mahidol University under the National Research University Initiative are acknowledged.

REFERENCES

- Tsunoyama, H.; Sakurai, H.; Negishi, Y.; Tsukuda, T. J. Am. Chem. Soc. 2005, 127, 9374.
- Tsunoyama, H.; Sakurai, H.; Ichikuni, N.; Negishi, Y.; Tsu-kuda, T. Langmuir 2004, 20, 11293.
- 3. Magdesieva, T. V.; Nikitin, O. M.; Levitsky, O. A.; Zinovyeva, V. A.; Bezverkhyy, I.; Zolotukhina, E. V.; Vorotyntsev, M. A. *J. Mol. Catal. A: Chem.* **2012**, *353*, 50.
- Kantam, M. L.; Roy, M.; Roy, S.; Sreedhar, B.; Madhavendra,
 S. S.; Choudary, B. M.; De, R. L. *Tetrahedron* 2007, 63, 8002.
- Cirtiu, C. M.; Dunlop-Briere, A. F.; Moores, A. Green Chem. 2011, 13, 288.
- 6. Adeli, M.; Mehdipour, E.; Bavadi, M. J. Appl. Polym. Sci. **2010**, 116, 2188.
- Somorjai, G. A.; Park, J. Y. Angew. Chem. Int. Ed. 2008, 47, 9212.
- Chaicharoenwimolkul, L.; Munmai, A.; Chairam, S.; Tewasekson, U.; Sapudom, S.; Lakliang, Y.; Somsook, E. *Tetrahedron Lett.* 2008, 49, 7299.
- 9. Skotheim, T. A.; Reynolds, J., Eds. Handbook of Conducting Polymer: Conjugated Polymers, Theory, Synthesis, Properties, and Characterization; CRC Press: New York, **2007**.
- Chen, Z.; Della Pina, C.; Falletta, E.; Lo Faro, M.; Pastaa, M.; Rossi, M.; Santo, N. J. Catal. 2008, 259, 1.
- 11. Cetin, A.; Ortiz-Colon, S.; Espe, M. P.; Ziegler, C. J. Dalton Trans. 2008, 64.
- 12. Han, C. C.; Lu, C. H.; Hong, S. P.; Yang, K. F. *Macromole-cules* **2003**, *36*, 7908.

- 13. Amaya, T.; Saio, D.; Koga, S.; Hirao, T. *Macromolecules* **2010**, *43*, 1175.
- 14. Kane-Maguire, L. A. P.; Wallace, G. G. Chem. Soc. Rev. **2010**, *39*, 2545.
- 15. Miyaura, N.; Suzuki, A. Chem. Rev. 1995, 95, 2457.
- 16. Diederich, F.; Stang, P. J., Eds. Metal-Catalyzed Cross-Coupling Reactions; Wiley-VCH: New York, 1998.
- 17. Marziale, A. N.; Faul, S. H.; Reiner, T.; Schneider, S.; Eppinger, J. *Green Chem.* **2010**, *12*, 35.
- 18. Dhara, K.; Sarkar, K.; Srimani, D.; Saha, S. K.; Chattopadhyay, P.; Bhaumik, A. *Dalton Trans.* **2010**, *39*, 6395.
- Nobre, S. M.; Monteiro, A. L. J. Mol. Catal. A Chem. 2009, 313, 65.
- Tamami, B.; Ghasemi, S. J. Mol. Catal. A Chem. 2010, 322, 98.
- Gallon, B. J.; Kojima, R. W.; Kaner, R. B.; Diaconescu, P. L. Angew. Chem. Int. Ed. 2007, 46, 7251.
- 22. Houdayer, A.; Schneider, R.; Billaud, D.; Ghanbaja, J.; Lambert, J. Appl. Organomet. Chem. 2005, 19, 1239.
- Budroni, G.; Corma, A.; Garia, H.; Primo, A. J. Catal. 2007, 251, 345.
- 24. Kwong, F. Y.; Chan, K. S.; Yeung, C. H.; Chan, A. S. C. *Chem. Commun.* **2004**, 2336.
- 25. Stepnicka, P.; Lamac, M.; Cisarova, I. *Polyhedron* **2004**, *23*, 921.
- Cousaert, N.; Toto, P.; Willand, N.; Deprez, B. Tetrahedron Lett. 2005, 46, 6529.
- Sliger, M. D.; Broker, G. A.; Griffin, S. T.; Rogers, R. D.;
 Shaughnessy, K. H. *J. Organomet. Chem.* 2005, 690, 1478.
- 28. Shi, J. C.; Yang, P. Y.; Tong, Q. S.; Wu, Y.; Peng, Y. J. Mol. Catal. A: Chem. 2006, 259, 7.
- Wang, H. X.; Wu, H. F.; Yang, X. L.; Ma, N.; Wan, L. Polyhedron 2007, 26, 3857.
- Punji, B.; Mague, J. T.; Balakrishna, M. S. *Inorg. Chem.* 2007, 46, 10268.
- 31. Kuhnert, J.; Lamac, M.; Demel, J.; Nicolai, A.; Lang, H.; Stepnicka, P. J. Mol. Catal. A Chem. 2008, 285, 41.
- 32. Garabatos-Perera, J. R.; Butenschon, H. J. Organomet. Chem. 2008, 693, 357.
- 33. Yu, S. B.; Hu, X. P.; Deng, J.; Huang, J. D.; Wang, D. Y.; Duan, Z. C.; Zheng, Z. *Tetrahedron Lett.* **2008**, 49, 1253.
- 34. Stepnicka, P.; Krupa, M.; Lamac, M.; Cisarova, I. *J. Organomet. Chem.* **2009**, 694, 2987.
- 35. Tauchman, J.; Cisarova, I.; Stepnicka, P. Organometallics 2009, 28, 3288.
- Schulz, J.; Cisarova, I.; Stepnicka, P. J. Organomet. Chem. 2009, 694, 2519.
- 37. Mu, B.; Li, T. S.; Li, C. H.; Liu, P. P.; Shang, W.; Wu, Y. J. *Tetrahedron* **2009**, *65*, 2599.
- 38. Stepnicka, P.; Schulz, J.; Klemann, T.; Siemeling, U.; Cisarova, I. *Organometallics* **2010**, *29*, 3187.
- Ren, G. R.; Cui, X. L.; Wu, Y. J. Eur. J. Org. Chem. 2010, 2372.



Applied Polymer

- Asaro, M. F.; Nakayama, I.; Wilson, R. B. J. Org. Chem. 1992, 57, 778.
- Savage, D.; Alley, S. R.; Gallagher, J. F.; Goel, A.; Kelly, P. N.;
 Kenny, P. T. M. *Inorg. Chem. Commun.* 2006, 9, 152.
- 42. Ali Shah, A. U. H.; Holze, R. Synth. Methods 2006, 156, 566.
- 43. Amaya, T.; Saio, D.; Hirao, T. Tetrahedron Lett. 2007, 48, 2729.
- 44. Scott, J. C.; Pfluger, P.; Krounbi, M. T.; Street, G. B. *Phys. Rev. B* **1983**, *28*, 2140.
- 45. Jeevananda, T.; Siddaramaiah; Seetharamu, S.; Saravanan, S.; D'Souza, L. *Synth. Methods* **2004**, *140*, 247.
- 46. Zhang, J.; Shan, D.; Mu, S. L. Polymer 2007, 48, 1269.
- Petersen, R.; Foucher, D. A.; Tang, A.-Z.; Lough, A.; Raju,
 N. P.; Greedan, J. E.; Manners, I. Chem. Mater. 1995, 7,
 2045.

- 48. Lee, H. Y.; Goodenough, J. B. J Solid State Chem. 1999, 144, 220.
- 49. Xu, Y.; Dai, L.; Chen, J.; Gal, J.-Y.; Wu, H. Eur. Polym. J. 2007, 43, 2072.
- Shi, J.; Tong, B.; Zhao, W.; Shen, J.; Zhi, J.; Dong, Y.; Haussler, M.; Lam, J. W. Y.; Tang, B. Z. *Macromolecules* 2007, 40, 5612.
- 51. EL Sayed, A. M.; Yamasaki, S.; Yamauchi, A. *J. Appl. Polym. Sci.* **2008**, *107*, 1678.
- Kahol, P. K.; Pendse, V.; Pinto, N. J.; Traore, M.; Stevenson, W. T. K.; McCormick, B. J.; Gundersen, J. N. *Phys. Rev. B* 1994, 50, 2809.
- 53. Braga, A. A. C.; Ujaque, G.; Maseras, F. *Organometallics* **2006**, *25*, 3647.





Esterification of Fatty Acid Catalyzed by Hydrothermally Stable Propylsulfonic Acidfunctionalized Mesoporous Silica SBA-15

Win Win Mar and Ekasith Somsook*

NANOCAST Laboratory, Center for Catalysis, Department of Chemistry and Center for Innovation in Chemistry, Faculty of Science, Mahidol University, 272 Rama VI Road, Bangkok 10400, Thailand.

Abstract: Propylsulfonic acid-functionalized mesoporous silica SBA-15 has been synthesized via one-step strategy at 130°C based on the co-condensation of TEOS and MPTMS in the presence of Pluronic 123 polymer and H_2O_2 in HCl aqueous solution. The synthesized solid exhibited hydrothermal stability in boiling water without significant change in textural properties. The catalytic performance of the synthesized solid was studied in the esterification of oleic acid with methanol. The experimental results revealed that the large mesopore structures of SBA-15-PrSO₃H solid synthesized at 130°C could favor a facile access of oleic acid to the acid sites, making the comparable activity to that of phenyl ethyl sulfonic acid functionalized silica and higher than that of dry amberlyst-15.

Key words: SBA-15-PrSO₃H, esterification, microporosity

1 INTRODUCTION

Due to the unique advantages such as higher stability, easier separation, better regenerability and enhanced selectivity, heterogeneous acid catalysts could be used as a potential substitute to homogeneous acid catalysts in the esterification of feedstocks containing a high level of free fatty acid. In addition, several drawbacks of downstream processing-product separation, purification, and neutralization associated with homogeneous catalysis could also be avoided, making the production process more economical. The excellent catalytic activities of heterogeneous acid catalysts in the esterification of free fatty acid were described by different authors^{1–3)}.

The large surface areas, flexible pore sizes, and accessible surface active sites with controllable densities, the organofunctionalized mesostructured materials have been considered for a wide range of catalytic reactions^{4,5)}. Mesoporous silica SBA-15 with well-ordered hexagonal arrays of cylindrical channel, pore sizes in the range of 20-300 Å with narrow pore size distribution, high surface area (500 - 1000 m²/g), pore wall thickness (30-50 Å) with a large number of silanol groups at the surface of its pore channel was feasible for the incorporation of organofunctional group⁶⁻⁸⁾ and the resulting organo-modified materials were tested in the esterification of large substrate molecules,

such as fatty acids and esters⁹⁻¹¹⁾. The covalent attachments of organosulfonic functional groups to the surface of the mesoporous materials could be achieved by two strategies-a post-synthesis grafting and one-step co-condensation methods¹²⁻¹⁴⁾. The hydrothermal stabilities of mesoporous silica^{16, 17)} and functionalized mesoporous silica^{16, 17)} are also important issues for various catalytic applications.

This study was aimed to evaluate the esterification activity of propyl sulfonic acid- functionalized mesoporous SBA-15 silica synthesized at $130\,^{\circ}\!\!\mathrm{C}$. In this work, SBA-15-PrSO_3H was prepared by the direct one-step strategy and the material was characterized by XRD, FT-IR, TGA, N_2 adsorption-desorption, TEM, and ion-exchange capacity. For activity comparison, phenylethylsulfonic acid-functionalized silica gel, and dry amberlyst-15 were also used. The reusability of the synthesized SBA-15-PrSO_3H solid was also conducted in order to evaluate the suitability of solid catalyst for esterification of free fatty acids.

2 EXPERIMENTAL SECTION

2.1 Materials and synthesis

SBA-15-PrSO $_3$ H was synthesized though the modification of the procedure described by D. Margolese *et al.* ¹⁸⁾: 4 g of

Accepted January 15, 2013 (received for review November 19, 2012)
Journal of Oleo Science ISSN 1345-8957 print / ISSN 1347-3352 online
http://www.jstage.jst.go.jp/browse/jos/ http://mc.manusriptcentral.com/jjocs

^{*}Correspondence to: Ekasith Somsook, NANOCAST Laboratory, Center for Catalysis, Department of Chemistry and Center for Innovation in Chemistry, Faculty of Science, Mahidol University, 272 Rama VI Road, Bangkok 10400, Thailand E-mail: ekasith.som@mahidol.ac.th

Pluronic P123 (Aldrich), a triblock copolymer [PEO₂₀- PPO_{70} - PEO_{20} , M.W. = 5800] and 125 cm³ of 1.9 mol/dm³ HCl was stirred at room temperature for 2 h until the clear solution had been obtained. After the subsequent heating of such solution to 40°C, 6.83 g of tetraethyl orthosilicate (TEOS, 98%, Aldrich) was added and hydrolyzed for an additional 3 hours. Following the prehydrolysis of TEOS, 1.61 g of (3-mercaptopropyl)-trimethoxysilane (MPTMS, 95%, Aldrich) and 8.36 g of aqueous solution of H₂O₂(30 wt%) were added at once and the mixture was maintained at 40°C for 20 hours under continuous stirring, corresponding to the molar ratio of 1SiO₂/0.249 MPTMS/0.0738 H₂O₂/6.97 HCl/173 H₂O with the molar ratio of MPTMS/ (MPTMS + TEOS) of 0.2 and that of $H_2O_2/MPTMS = 9$. The reaction mixture was then aged at 130°C for 24 hours under static condition in a Teflon-lined steel autoclave in order to limit the microporosity of the solid materials reported by A. Galarneau et al. 19). The solid product was recovered by filtration, washing with ethanol, and oven-drying. For the elimination of the surfactant, 1 g of solid was extracted with 200 cm³ of a mixture of 15:1 (wt/wt) EtOH/ HCl(37 wt%) under reflux for 24 hours. The extracted solid was then oven-dried and stored as SBA-15-PrSO₃H. In order to know the extent of microporosity, aging of the reaction mixture was also performed at 100°C and the solid obtained was denoted as SBA-15-PrSO₃H(100° C)¹⁸⁾.

2.2 Other solid acids

For the activity comparison of the mentioned catalyst, the phenylethyl- SO_3H silica material was also prepared according to the procedure as described by Melero *et. al.*²⁰⁾ using a Grace Davison silica (G5H) support and 2-(4-chlorosulfonylphenyl) ethyltrimethoxysilane (CSPTMS) as grafting species. The G5H material is a mesoporous silica with a very narrow pore size distribution centered around 16 nm and a surface area of 513 m²/g. Dry amberlyst-15(0.3-1mm, Rhom-Hass) was also used to compare their performances in esterification reaction.

2.3 Characterization

Powder X-ray diffraction (XRD) patterns (2θ range from 0.5 to 6° with a resolution of 0.02°) were performed on a D8 ADVANCE BRUKER AXS diffractometer using Cu $K\alpha$ radiation. Transmission electron microscopy (TEM) images were obtained using a JEOL 1200 EXII electron microscope operating at 120 kV. Nitrogen adsorption and desorption isotherms at -196°C were collected using a micromeritics TriStar 3000 unit. All samples were degassed at 120°C for 6 hours before measurements. The surface area was calculated by the BET method and pore diameters were determined from the nitrogen desorption branch by the Broekhoff and de Boer (BdB) method, respectively. Thermogravimetric analysis (TGA) were carried out on a NETZSCH TG 209 apparatus at a heating rate of 10°C/min

from 25 to 900°C under air flow. Ion-exchange capacities of samples were determined using aqueous solutions of sodium chloride 2 mol/dm³ as exchange agents. In a typical experiment, 0.05 g of solid was added to 10 g of 2 mol/dm³ NaCl aqueous solution and stirred for 15 hours to equilibrate and thereafter titrated by dropwise addition of 0.01 mol/dm³ NaOH aqueous solution with phenolphthalein as indicator. From the volume of titrant solution, the acid exchange capacity was determined in units of meq H+/g of solid¹⁸⁾. Fourier-transform Infrared diffuse reflectance spectra(DRIFT) were recorded on a Bruker Equinox 55 spectrophotometer, at room temperature, in the range 4000-1000 cm⁻¹ (resolution 4 cm⁻¹, 32 scans). Catalyst samples are diluted in KBr. The estimation of the hydrothermal stability of the synthesized SBA-15-PrSO₃H solids was conducted by refluxing the solids in deionized water (0.5 g of solid/0.5 L of water) for 1 day. The solids were recovered by filtration and oven-drying.

2.4 Catalytic activity tests

All the liquid-phase esterification reactions were conducted in a 100 cm³ two-necked flask equipped with a water-cooled reflux condenser in a thermostatic oil bath with a magnetic stirrer. In the typical experiment, the reaction mixture of oleic acid (5 g) to methanol (5.66 g) and 2 wt% of catalyst referred to oleic acid was used with a fixed stirring rate of 600 rpm at 60°C in air. Unless otherwise specified, all kinetic reactions were performed at 60°C and all solid acid catalysts were activated prior to esterification. Firstly, the mixture of the desired molar ratio of oleic acid to methanol was pre-heated while stirring. Once the required temperature was achieved, the esterification reaction was started by charging the catalyst (t = 0) of the reaction). The periodically withdrawn samples were filtered and injected by using a microscale syringe (1×1) in a Varian 3900 gas chromatograph, equipped with a flame ionization detector and a HP-5 capillary column (30 m× 0.32 mm i.d, 0.25 µm film thickness) and hydrogen gas as a carrier gas at 1 ml/min. $T_{injector} = 280^{\circ}C$, $T_{detector} = 285^{\circ}C$. The oven temperature was programmed from 180 to 280°C with a rate of 10°C/min and then 2 minutes isothermal conditions were applied. The methyl oleate yield was calculated by the calibration curve. The aim of the standardization is to quantify the product (in mol) formed during the esterification reaction. In order to standardize the methyl oleate, four methyl oleate solutions at different concentrations in the range of 0.125 mol/dm³ to 1 mol/dm³, in methanol have been prepared by successive dilution and injected in gas chromatograph. The ratio (area of methyl oleate peak)/ (area of methanol peak) or A1/A2 is calculated and then, the graph A1/A2 versus[methyl oleate] is drawn, assuming constant the methanol concentration (solvent).

Consequently, the response coefficient is the slope of the straight line.

 $A_1/A_2 = \alpha$ [methyl oleate]

where α = response coefficient for methyl oleate.

The area ratio of methanol to methyl oleate from the chromatogram and α obtained from the calibration curve were used in order to calculate the methyl oleate concentration as follows:

- (1) [methyl oleate] = $(A_1/A_2)/\alpha$ = a mmol/cm³ Methyl oleate concentration can be expressed in mmol,
- (2) mmol of methyl oleate = a mmol/cm³ × volume of reaction mixture in cm³

= b mmol

Alternatively, the percent Yield of methyl oleate can also be calculated:

(3) Yield of methyl oleate (%) = b/initial mmol of oleic acid \times 100

3 RESULTS AND DISCUSSION

3.1 Characterization of sulfonic acid-functionalized mesoporous silicas

The low angle XRD patterns of SBA-15-PrSO₃H samples (as-synthesized and after surfactant extraction) were depicted as shown in Fig. 1. Three well-resolved characteristic d(100), d(110) and d(200) peaks of p6mm 2D hexagonal structure confirm the presence of SBA-15 mesophases with 2D hexagonal symmetry for both samples. The intensity of the (100) reflection of extracted solid with d-spacing 11.3 nm increased in comparison to that of as-synthesized one, indicating a better ordered mesoporous structure for SBA-15-PrSO₃H material after surfactant removal.

The TEM images also confirm the uniform and well-ordered mesostructure with a hexagonal symmetry (p6mm)of the typical honeycomb appearance of SBA-15 material as in Fig. 2. The nitrogen adsorption-desorption isotherms at -196° C of different sulfonic-modified mesoporous silica are reported in Fig. 3. Both isotherms are of characteristic type IV with H1 type hysteresis loops according to the IUPAC classification, exhibiting sharp step hysteresis loops of typical mesoporous materials including pores of constant cross-section with narrow pore size distribution. The absorbate uptake of SBA-15-PrSO₃H at the low relative pressure region was higher than that of phenylethyl mesoporous silica material, corresponding to a higher surface area with larger pore volume measuring at the top of the filling step. Even using large MPTMS loading in the sample, the large pore volume and S_{BET} of SBA-15-PrSO $_3$ H could be achieved with the indication of the important role of synthe sized temperature at 130° C, removing the micropores with simultaneous development of mesopores for easy attachement of organo functional groups during the catalyst synthesis.

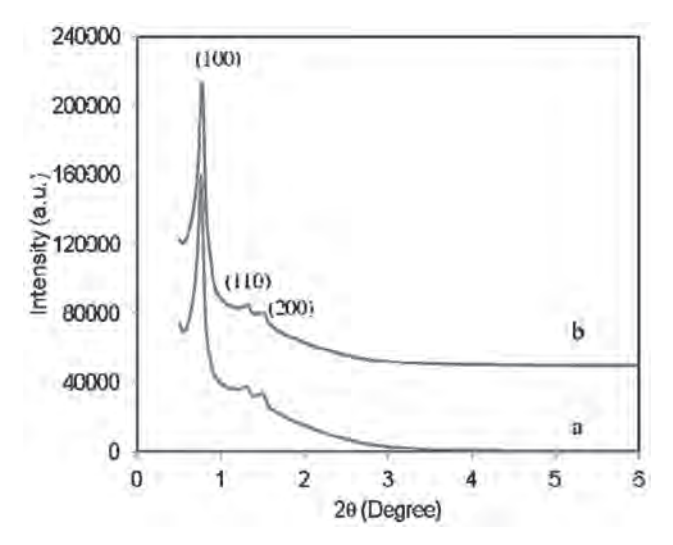


Fig. 1 XRD patterns of (a) as-synth SBA-15-PrSO₃H (b) SBA-15-PrSO₃H.

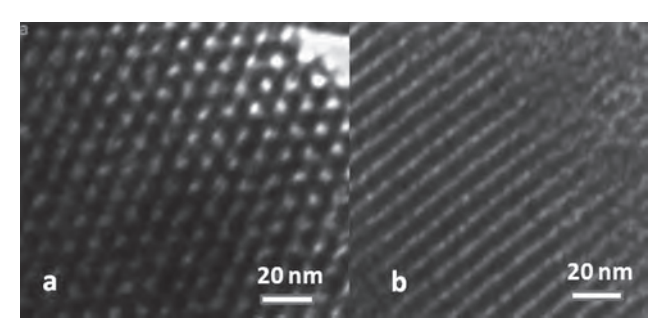


Fig. 2 Transmission electron micrograph (TEM) images of SBA-15-PrSO₃H (a) Perpendicular to the channel axis (b) parallel to the channel axis.

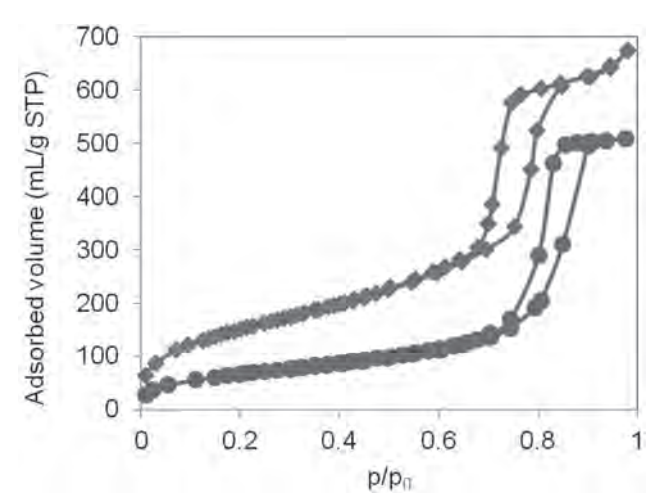


Fig. 3 N₂ isotherms of ♠: SBA-15-PrSO₃H ♠ PhEtSO₃H silica materials.

The amount of incorporated organic functional groups was determined by thermogravimetric analysis on samples under air flow as shown in Fig. 4. The TGA thermograms

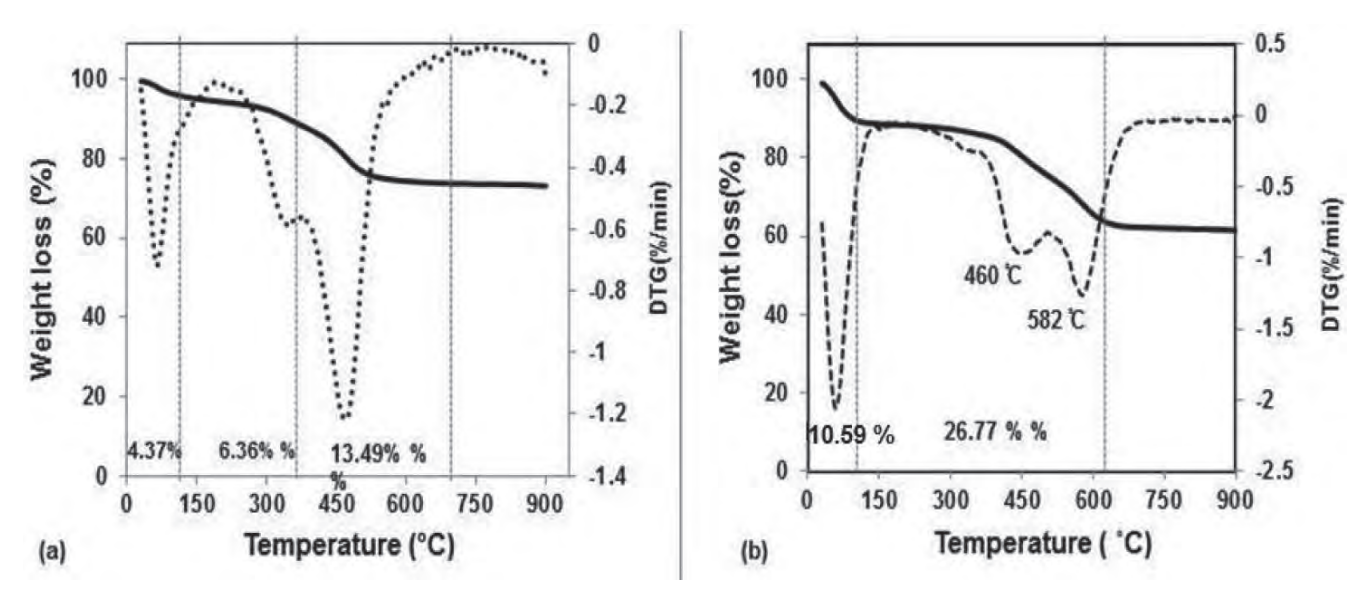


Fig. 4 TGA and DTG profiles of sulfonic acid-functionalized silicas (a) SBA-15-PrSO₃H (b) PhEtSO₃H silica.

Table 1 Textural and structural properties of different sulfonic acid functionalized solid materials.

	Textural properties					XRD	
Catalyst	S_{BET} (m^2/g)	mesopore volume (mL/g)	micropore volume (mL/g)	pore diameter (nm)	wall thickness (nm)	d100 (nm)	a ₀ (nm)
SBA-15-PrSO ₃ H	713	0.96	0.030	9.0	4.7	11.3	13.1
SBA-15-PrSO ₃ H-HT	692	0.94	0.003	8.4	5.4	11.6	13.4
SBA-15-PrSO ₃ H (100 C)	743	0.65	0.060	5.7	6.1	9.9	11.5
SBA-15-PrSO ₃ H (100 C)-HT	523	0.43	0.020	3.6	7.4	9.7	11.2
PhEtSO₃H silica	440	0.79	_	13.2	_	_	
Amberlyst- 15(dry)	53	0.40	_	30	_	_	

d-Spacing (d_{100}) measured by small-angle XRD, ($\lambda = \text{nd}_{100} \sin \theta$)

cell parameter (a_0) by $a = 2 d_{100} / \sqrt{3}$,

Wall thickness by $t = a - 0.95 D_{BdB}$, and

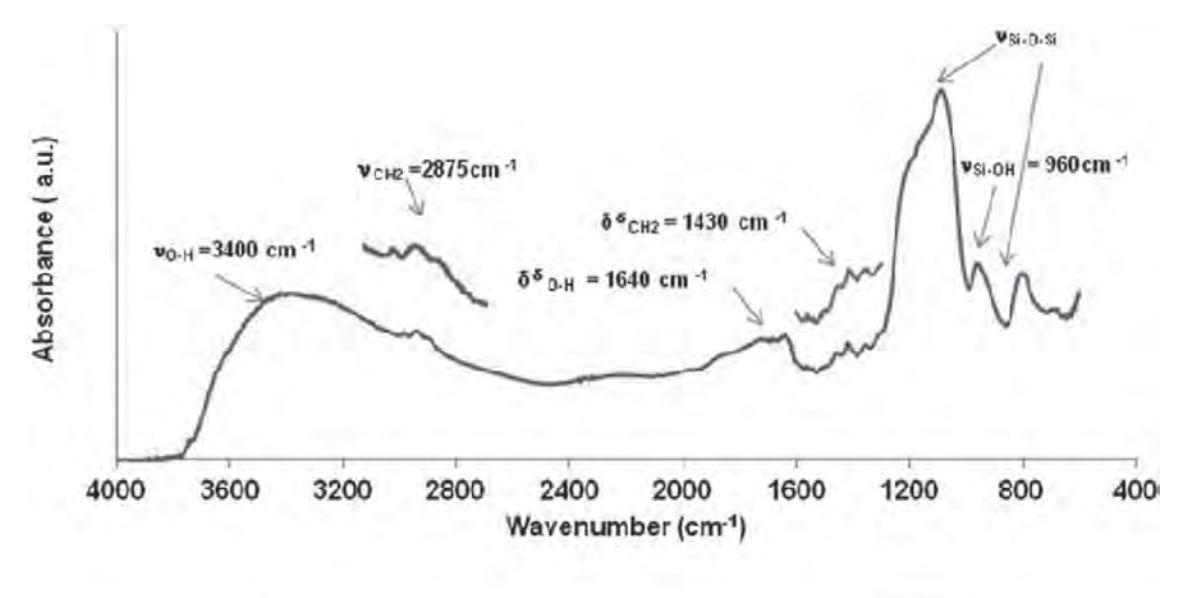
HT = hydrothermal treatment sample

show the first peak lower than 100°C due to the desorption of water followed by an intense broad peaks between 400-600°C corresponding to the decomposition of sulfonic acid group. In the thermogram of SBA-15-Pr-SO₃H, absorption peak between 130°C and 350°C is related to the loss of remaining surfactant molecules, unoxidized thiol groups, and ethoxy groups adsorbed on the solid surface during the surfactant extraction process by acidic-ethanol mixture²¹⁾. Thus, the organic composition in the SBA-15-PrSO₃H material was ca.1.9 mmol/g of solid which was lower than the reported value $(ca.2.12 \text{ mmol/g})^{18)}$.

In order to determine the accessibility of sulfonic acid in the functionalized materials, ion-exchange capacities taken by acid-base titration $^{18)}$ are shown in Table 1. The acid exchange capacity of PhEtSO $_3$ H silica (1.5 milliequivalent H $^+$ / $g_{catalyst}$) is in good agreement with that of TGA result (1.6 mmol/gcatalyst). In contrast, larger acid site density of SBA-15-PrSO $_3$ H solid determined by TGA could be explained the presence of some extent of unoxidized thiol group/par-

tially oxidized disulphides or remaining organic parts in the materials. It was also observed that the acid densities of dry amberlyst-15 coincided between ion-exchnage technique and supplier's results.

The textural, and structural properties of sulfonic-functionalized samples were summarized in Table 1. From the textural properties of SBA-15-PrSO₃H synthesized at $130\,^{\circ}\mathrm{C}$, micropores are empty compared to that of solid synthesized at $100\,^{\circ}\mathrm{C}$, indicating the limited microporosity at higher synthesis temperature. The pore wall thickness of SBA-15-PrSO₃H synthesized at $130\,^{\circ}\mathrm{C}$ was also found to be 4.7 nm. The S_{BET} of PhEtSO₃H silica was of 440 m²/g corresponding to the parent silica support with S_{BET} of $513\,$ m²/g, indicating the incorporation of sulfonic group to the silica support. The commercial cation-exchange resin, dry amberlyst-15 is a gel type structure of microspheres that forms a macroporous polymer and composed of copolymer divinyl benzene-styrene with sulfonic acid group (4.7 milliequivalent/g). The macroreticular structure is character-



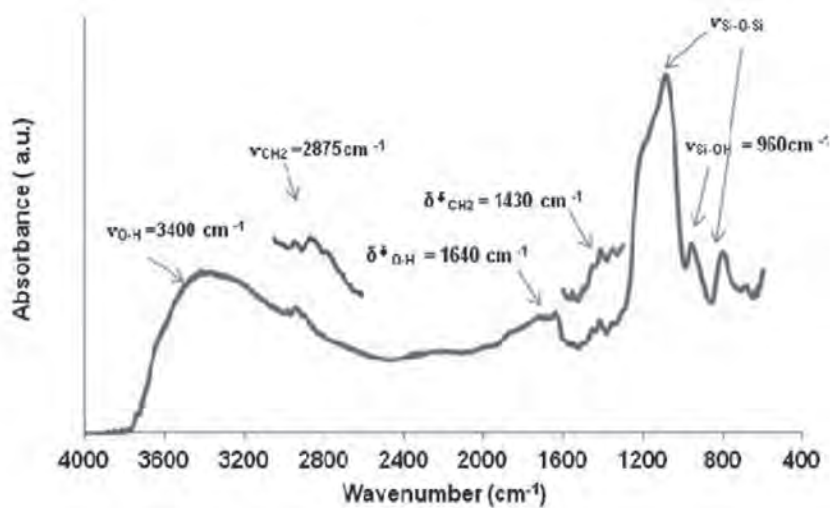


Fig. 5 FT-IR of SBA-15-PrSO₃H.

Table 2 Acid sites and catalytic activities in esterification of oleic acid with methanol of sulfonic acid functionalized materials indicating initial rates and turn over frequencies.

Catalyst	Initial rate, r ₀ (mmol/min/g _{cata})	acid site (mequi H ⁺ /g)	TOF (min ⁻¹)
SBA-15-PrSO ₃ H	2.2	1.4	1.6
PhEtSO₃H silica	2.35	1.5	1.6
Amberlyst-15 (dry)	1.15	4.7	0.2

ized by a surface area of 53 m²/g, an average pore diameter of 30 nm and a porous volume of 0.40 cm³/g. After the hydrothermal treatment, the textural properties of SBA-15-PrSO $_{\!3}H$ synthesized at $130\,^{\circ}\!\!\mathrm{C}$ were not significantly changed, showing the good hydrothermal stability compared to those of solid synthesized at $100\,^{\circ}\!\!\mathrm{C}$.

As shown in Fig. 5, FT-IR spectrum of SBA-15-PrSO₃H solid qualititatively identified the organic functional groups

 $\nu_{\text{CH2}}\!=\!2875~\text{cm}^{-1}$ of the propyl chain and others deformation bands in the region 1430 cm $^{-1}$, confirming the presence of propyl group on the parent silica support. The absorption peaks at $\nu_{\text{OH}}\!=\!3450~\text{cm}^{-1}$ and $\delta_{\text{OH}}\!=\!1650~\text{cm}^{-1}$ are assigned to the adsorbed water on the solid. The absorption bands 1070 and 800 cm $^{-1}$ were observed for the typical Si-O-Si bands of condensed SiO $_2$ network and $\nu_{\text{Si-OH}}\!=\!960~\text{cm}^{-1}$ is associated with the non-condensed Si-OH

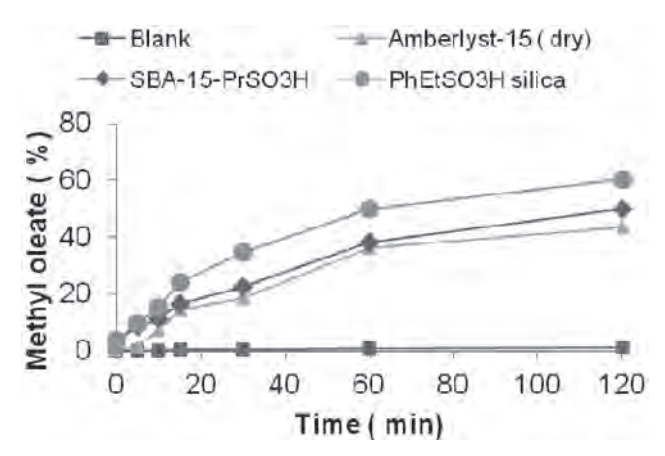


Fig. 6 Esterifications of oleic acid with MeOH as a function of reaction period at 60°C over (a) ■: blank (b) ◆: SBA-15-PrSO₃H (c) ●: PhEt-SO₃H silica (d) ▲: Amberlyst15 as catalysts.

stretching band²²⁾. The weak peaks in the low frequency region 1300-1500 cm⁻¹ and 2800-3000 cm⁻¹ are probably from the C-H stretching bands of ethoxy group from ethanol used during template extraction²³⁾. The absorption peak associated with the S-H band could not clearly be seen due to the lower absorption coefficient of the $\nu_{\rm S-H}$.

3.2 Cataytic activity tests of sulfonic acid-functionalized mesoporous silicas

The experimental results obtained from the assessement of catlytic performance of the sulfonic acid-functionalized solids in the esterification of oleic acid with methanol are shown in Table 2 and Fig. 6. The excess methanol was practically used in the esterification reaction to put forward the reaction equilibrium to the product side. From the GC analysis of the periodically withdrawn samples, methyl oleate was observed as only one product. The initial rates were determined during the first 10-30 minutes of the reaction, corresponding to the quantity of methyl oleate (< 10 mol%). Autocatalysis of oleic acid is quite slow in the reaction, giving 1% yield of methyl oleate for 2 hours. In addition, the unloaded SBA-15 also showed the low activity giving 1% after 2 hours. The incorporation of an electronwithdrawing phenyl group with the sulfonic acid group to the PhEtSO₃H silica soilds exhibited higher acid strength with higher methyl oleate conversion than that of SBA-15-PrSO₃H silica material²⁴⁾. However, the turnover frequency (TOF) of SBA-15-PrSO₃H is identical to that of PhEtSO₃H silica suggesting that bulky oleic acid molecule could easily access to the active sites in the reasonable large mesopores of SBA-15-PrSO₃H. Amberlyst-15, an ionexchange resin, is commonly used for esterification and transesterification reactions. Activation of amberlyst was carried out, following the procedure described by Wainwright et al²⁵⁾. The catalyst is washed in distilled water and

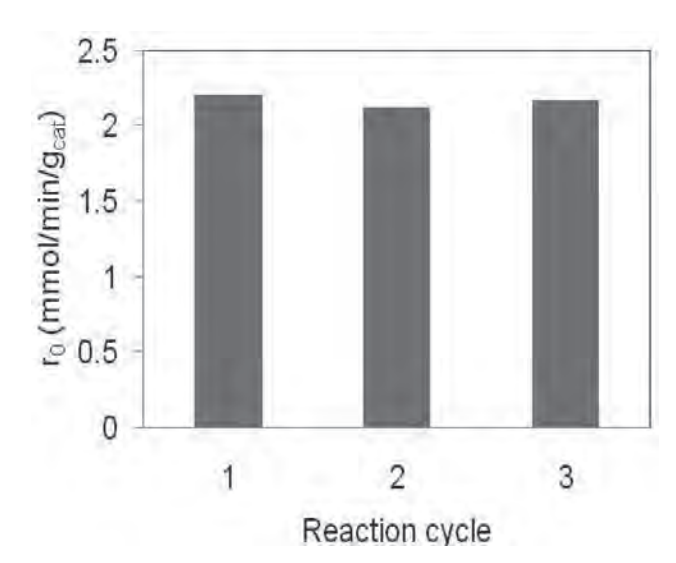


Fig. 7 Catalyst recycle experiments of SBA-15-Pr-SO₃H. on oleic acid conversion on (10;1) molar ratio of oleic acid to methanol, 60°C, 2 wt % catalyst.

dried at 100° C for 4 hours. Then it is put in 10 wt% sulfuric acid solution for 2 hours and afterwards, it is washed with water until neutrality and dried at 100° C before use. An interesting study²⁶⁾ shows that the resistance of the internal diffusion is important with particles greater than 0.125 mm. Consequently, the internal diffusion resistance is significant in commercial particle sizes of amberlyst-15(0.3-1 mm). In addition, the low activity could also be attributed to the difficult accessibility of fatty acid substrate to the active²⁴⁾.

Influence of the mass of catalyst SBA-15-PrSO₃H was studied in esterification reaction by charging different catalyst loadings into the reaction vessel. The results demonstracted that the initial rate doubles when the catalyst mass doubles, suggesting that the reaction is not limited by mass transfer. The initial rate is proportional to the acidic sites concentration. The sulfonated mesoporous silica SBA-15-PrSO₃H was used in repeated runs. After reaction, the catalyst is filtered and washed with ethanol. The recycled solid is stirred in ethanol for 4 hours two times, oven-dried at 80° C and then used for the next reaction. The reaction is tested up to three recycles and no-decrease in the initial rate is observed as shown in Fig. 7.

4 CONCLUSIONS

Propylsulfonic acid-functionalized mesoporous silica SBA-15 has been synthesized via the direct one-step synthesis. The experimental results revealed that the intrinsic per site activity of synthesized propylsulfonic-functionalized SBA-15 solid could be comparable to that of phenyl

ethyl sulfonic acid functionalized silica and higher than that of commercial sulfonic acid solid, dry amberlyst-15, due to an easy accessment of oleic acid substrate molecule to the acid sites attached to reasonable large mesopores of SBA-15-PrSO $_3$ H solid synthesized at $130\,^{\circ}\mathrm{C}$. Besides, the hydrothermal and operational stability of SBA-15-PrSO $_3$ H solid partially ascribed to the contribution of thick pore wall as well as the propyl group present in the hybrid material.

5 ACKNOWLEDGEMENTS:

The authors acknowledge the Royal Golden Jubilee Program (RGJ), TICA (Thailand International Development Cooperation Agency), and the French Embassy in Thailand through the assistance of Prof. François Fajula for a Ph.D. scholarship and the Biofuel Development for Thailand fund through The Center of Excellence for Innovation in Chemistry (PERCH-CIC), the Thailand Research Fund-the Office of the Higher Education (RMU5380043), the S&T Postgraduate Education and Research Development Office (PERDO), The Commission on Higher Education (CHE), Thailand for financial support.

REFERENCES:

- 1) Morales, G.; van Grieken, R.; Martín, A.; Martínez, F. Sulfonated polystyrene-modified mesoporous organosilicas for acid-catalyzed processes. *Chem. Eng. J.* **161**, 388-396 (2010).
- 2) Takagaki, A.; Toda, M.; Okamura, M.; Kondo, J. N.; Hayashi, S.; Domen, K.; Hara, M. Esterification of higher fatty acids by a novel strong solid acid. *Catal. Today* **116**, 157-161 (2006).
- Marchetti, J. M.; Miguel, V. U.; Errazu, A. F. Heterogeneous esterification of oil with high amount of free fatty acids. *Fuel* 86, 906-910 (2007).
- 4) Zhao, D.; Huo, Q.; Feng, J.; Chmelka, B. F.; Stucky, G. D. Nonionic Triblock and Star Diblock Copolymer and Oligomeric Surfactant Syntheses of Highly Ordered, Hydrothermally Stable, Mesoporous Silica Structures. J. Am. Chem. Soc. 120, 6024-6036 (1998).
- Dufaud, V.; Davis, M. E. Design of Heterogeneous Catalysts via Multiple Active Site Positioning in Organic-Inorganic Hybrid Materials. J. Am. Chem. Soc. 125, 9403-9413 (2003).
- 6) Kruk, M.; Jaroniec, M.; Ko, C. H.; Ryoo, R. Characterization of the Porous Structure of SBA-15. *Chem. Mater.* **12**, 1961-1968 (2000).
- 7) Galarneau, A.; Cambon, H.; Di Renzo, F.; Ryoo, R.; Choi, M.; Fajula, F. Microporosity and connections between pores in SBA-15 mesostructured silicas as a

- function of the temperature of synthesis. New J. Chem. 27,73-79(2003).
- 8) Zhao, D.; Feng, J.; Huo, Q.; Melosh, N.; Fredrickson, G. H.; Chmelka, B. F.; Stucky, G. D. Triblock Copolymer Syntheses of Mesoporous Silica with Periodic 50 to 300 Angstrom Pores. *Science* **279**, 548-552 (1998).
- Mbaraka, I. K.; Shanks, B. H. Design of multifunctionalized mesoporous silicas for esterification of fatty acid. J. Catal. 229, 365-373 (2005).
- Miao, S.; Shanks, B. H. Esterification of biomass pyrolysis model acids over sulfonic acid-functionalized mesoporous silicas. *Appl. Catal. A: General* 359, 113-120 (2009).
- 11) Karam, A.; Gu, Y.; Jerome, F.; Douliez, J.-P.; Barrault, J. Significant enhancement on selectivity in silica supported sulfonic acids catalyzed reactions. *Chem. Commun.* 2222-2224 (2007).
- 12) Hoffmann, F.; Cornelius, M.; Morell, J.; Fröba, M. Silica-Based Mesoporous Organic-Inorganic Hybrid Materials. *Angew. Chem. Int. Ed.* **45**, 3216-3251 (2006).
- 13) Van Rhijn, M. W.; De Vos, E. D.; Sels, F. B.; Bossaert, D. W., Sulfonic acid functionalised ordered mesoporous materials as catalysts for condensation and esterification reactions. *Chem. Commun.* 317-318 (1998).
- 14) Feng, X.; Fryxell, G. E.; Wang, L.-Q.; Kim, A. Y.; Liu, J.; Kemner, K. M. Functionalized Monolayers on Ordered Mesoporous Supports. *Science* 276, 923-926 (1997).
- 15) AlOthman, Z. A.; Apblett, A. W. Synthesis and characterization of a hexagonal mesoporous silica with enhanced thermal and hydrothermal stabilities. *Appl. Surf. Sci.* 256, 3573-3580 (2010).
- 16) Liu, J.; Yang, Q.; Kapoor, M. P.; Setoyama, N.; Inagaki, S.; Yang, J.; Zhang, L. Structural Relation Properties of Hydrothermally Stable Functionalized Mesoporous Organosilicas and Catalysis. J. Phys. Chem. B 109, 12250-12256 (2005).
- 17) Yang, Q.; Li, Y.; Zhang, L.; Yang, J.; Liu, J.; Li, C. Hydrothermal Stability and Catalytic Activity of Aluminum-Containing Mesoporous Ethane-Silicas. *J. Phys. Chem. B* **108**, 7934-7937 (2004).
- 18) Margolese, D.; Melero, J. A.; Christiansen, S. C.; Chmelka, B. F.; Stucky, G. D. Direct Syntheses of Ordered SBA-15 Mesoporous Silica Containing Sulfonic Acid Groups. *Chem. Mater.* **12**, 2448-2459 (2000).
- 19) Galarneau, A.; Nader, M.; Guenneau, F.; Di Renzo, F.; Gedeon, A. Understanding the Stability in Water of Mesoporous SBA-15 and MCM-41. J. Phys. Chem. C 111, 8268-8277 (2007).
- 20) Melero, J. A.; Stucky, G. D.; van Grieken, R.; Morales, G. Direct syntheses of ordered SBA-15 mesoporous materials containing arenesulfonic acid groups. *J. Mater. Chem.* 12, 1664-1670 (2002).
- 21) Melero, J. A.; Bautista, L. F.; Morales, G.; Iglesias, J.; Sánchez-Vázquez, R. Biodiesel production from crude

- palm oil using sulfonic acid-modified mesostructured catalysts. *Chem. Eng. J.* **161**, 323-331 (2010).
- 22) Wang, X.; Cheng, S.; Chan, J. C. C. Propylsulfonic Acid-Functionalized Mesoporous Silica Synthesized by in Situ Oxidation of Thiol Groups under Template-Free Condition. J. Phys. Chem. C 111, 2156-2164 (2007).
- 23) Sartori, G.; Bigi, F.; Maggi, R.; Sartorio, R.; Macquarrie, D. J.; Lenarda, M.; Storaro, L.; Coluccia, S.; Martra, G. Catalytic activity of aminopropyl xerogels in the selective synthesis of (E)-nitrostyrenes from nitroalkanes and aromatic aldehydes. J. Catal. 222, 410-418 (2004).
- 24) Mbaraka, I. K.; Radu, D. R.; Lin, V. S. Y.; Shanks, B. H. Organosulfonic acid-functionalized mesoporous silicas for the esterification of fatty acid. *J. Catal.* **219**, 329-336 (2003).
- 25) Zhang, C. M.; Adesina, A. A.; Wainwright, M. S. Isobutene hydration over Amberlyst-15 in a slurry reactor. *Chem. Eng. Process* **42**, 985-991 (2003).
- 26) Aragon, J. M.; Vegas, J. M. R.; Jodra, L. G. Self-Condensation of Cyclohexanone Catalyzed by Amberlyst-15. Study of Diffusional Resistances and Deactivation of the Catalyst. *Ind. Eng. Chem. Res.* 33, 592-599 (1994).